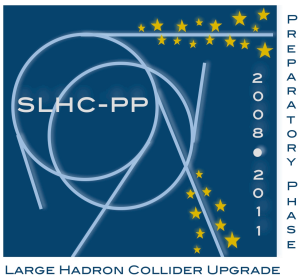

SLHC-PP

DELIVERABLE REPORT

EU DELIVERABLE: 7.2.1

Document identifier:	**SLHC-PP-7.2.1-982421-v1.0**
Contractual Date of Delivery to the EC	**End of Month 12 (March 2009)**
Actual Date of Delivery to the EC	**01/02/2011**
Document date:	**Part A: 31/3/2009 PART B: 30/11/2010**
Deliverable Title:	**In depth characterization of the two tuners plus cavities developed in the frame of the "HIPPI" JRA , FP6 (tuner/cavity characteristics)**
Work package:	**WP7: Development of critical components for the injectors**
Lead Beneficiary:	
Authors:	**PART A: R. Paparella, A. Bosotti, P. Pierini** **PART B: G. Devanz, M. Desmons, O. Piquet, J.-P. Charrier, A. Hamdi, E. Jacques, Y. Gasser, Y. Boudigou, D. Roudier, P. Sahuquet, D. Braud, W. Hofle, D. Valuch**
Document status:	
Document link:	https://edms.cern.ch/document/982421/1

History of Changes

Version	Date	Comment	Authors
1.0	-	-	-

The Preparatory Phase of the Large Hadron Collider upgrade (SLHC-PP) is a project co-funded by the European Commission in its 7th Framework Programme under the Grant Agreement n° 212114. SLHC-PP began in April 2008 and will run for 3 years.

TABLE OF CONTENTS

1. PART A 4

1.1. ---. EXECUTIVE SUMMARY 4
1.2. INTRODUCTION 4
1.3. CHARACTERIZATION OF THE INFN CAVITY/TUNER IN WARM CONDITION 4
1.4. RESULTS 6
1.4.1. Cavity Elastic Behavior And Frequency Sensitivity 6
1.4.2. Slow tuning range 8
1.4.3. Static piezo action 9
1.4.4. Considerations on Piezo Dynamic Behavior 10
1.4.5. Pressure Tests 11
1.5. CONCLUSIONS 13
1.6. REFERENCES 13

2. PART B 14

2.1. EXECUTIVE SUMMARY 14
2.2. INTRODUCTION 14
2.3. THE BETA 0.5 SACLAY CAVITY 15
2.4. PRELIMINARY MEASUREMENTS ON THE CAVITY 17
2.4.1. Room temperature measurements 17
2.4.2. Vertical cryostat CW measurements 19
2.4.3. 4.3 Horizontal test in CW 20
2.5. THE FAST PIEZO TUNER 21
2.6. PREPARATION AND INSTALLATION OF THE FULLY EQUIPPED CAVITY IN CRYHOLAB 23
2.6.1. 6.1 Coupler and cavity assembly 23
2.6.2. Cryholab test configuration 25
2.7. LOW POWER TESTS IN HORIZONTAL CRYOSTAT 27
2.7.1. Qext measurements 27
2.7.2. Tuning system characterization 28
2.7.3. Piezo to detuning transfer function 29
2.8. HIGH POWER TESTS 30
2.8.1. The pulsed RF power source 31
2.8.2. RF Pulse generation and control 31
2.8.3. Power coupler performance 32
2.8.4. Cavity behavior in pulsed mode 35
2.9. LORENTZ FORCE DETUNING COMPENSATION 37
2.10. PIEZO SIGNAL ANALYSIS 40
2.10.1. Time Domain signals 40
2.10.2. Spectral analysis 41
2.11. CONCLUSION 44
2.12. REFERENCES 45

1. PART A

1.1. ---. EXECUTIVE SUMMARY

We report here the activities for the characterization of the INFN cavity/tuner hardware performed in order to prepare the testing of the hardware in the CRYHOLAB at CEA Saclay.

1.2. INTRODUCTION

The INFN TRASCO Cavity and tuner design have been extensively reported in several deliverables of the CARE-HIPPI FP6 program [1.1-1.3]. A characterization of the cavity/tuner system in CRYHOLAB operating conditions is one of the objectives of task 7.2 of WP 7 of SLHC-PP. Since currently the CRYHOLAB horizontal test station is still being used for a thorough testing of the CEA cavity/tuner, and it will not become available for the assembly of the INFN cavity before summer 2010, it was agreed to perform and summarize in this short note a characterization of the system in warm conditions (to the maximum possible extent) in the piezo tuner test stand at INFN-LASA.

1.3. CHARACTERIZATION OF THE INFN CAVITY/TUNER IN WARM CONDITION

The tuner has been completely assembled on the Z502 TRASCO cavity and equipped with a motor unit and gearbox capable of operating at warm temperature in atmospheric condition, thus protecting from damage the assembly that will be used at later stages during the cryogenic testing in CRYHOLAB. The motor unit used for the warm test is a Phytron motor with the same characteristics of the VSS unit available for the cold tests and the gearbox is a standard, uncoated, set from Harmonic Drive, again with the same structural characteristics of the system prepared for the cold tests apart from a slightly higher reduction ratio (100 vs. 88 for the cold system). This latter aspect does not affect the characterization, anyway the reference variable for the tuning performances analyses has been chosen to be number of turns of the motor spindle, that is independent from the actual unit configuration. The fast tuner action is provided by two long piezo stacks from Noliac (dimensions 15x15x70 mm), the same device that will be used at cold.

The cavity has been equipped with an antenna at the main coupler port to excite the RF field close to the critical coupling conditions and a field probe at the cavity pickup port ($Q_{ext} \approx 10^{10}$). RF signals are monitored with a Vector Network Analyzer.

The motor unit is driven with a Phytron MCC-1 Driver unit and the piezo stacks are fed by a Piezomechanik amplifier capable to achieve their maximum nominal polarization of 200 V. Stepper motor driving equipment is interfaced with a PC to remotely drive the tuning operation with the same specific settings that will be used at cold (excitation frequency of 800 Hz, 1 A run current and 0 A stop current).

The characterization activities have been aimed to derive:

- The overall tuning range and cavity related tuning parameters.
- The static piezo response
- The behavior of the cavity with respect to the He pressure conditions
- The mechanical characteristics of the tuner (mainly the stiffness provided to the cavity in operating conditions).

Figure 1.1 shows the test bench at INFN-LASA, which makes use of the cavity field flatness tuning device. The cavity is supported at the flanges.

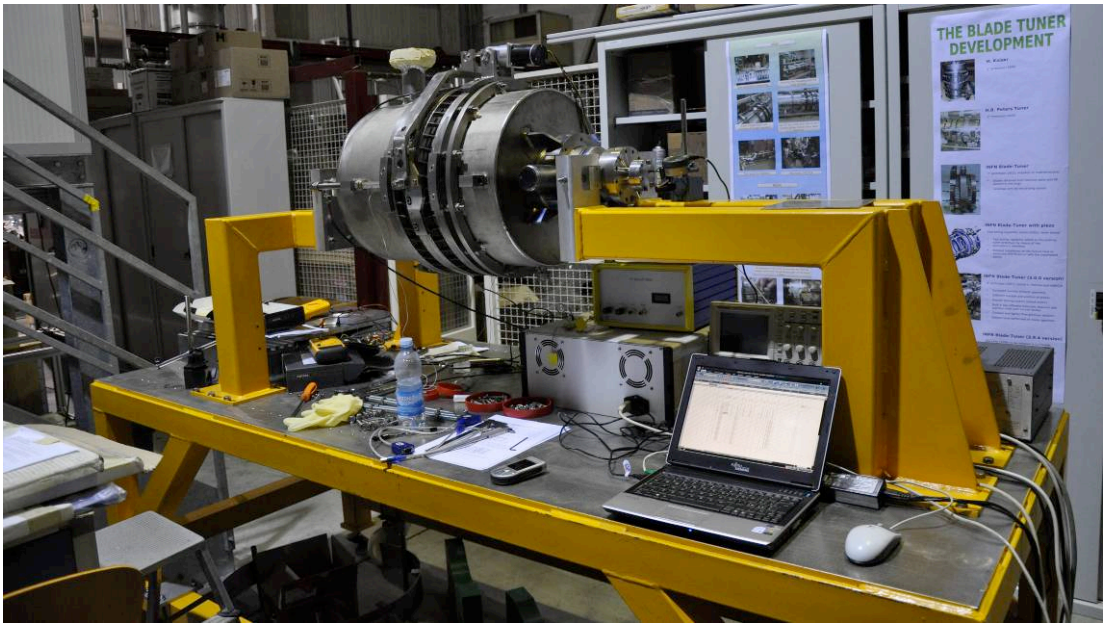

Figure 1.1: The cavity test bench at LASA.

Figure 1.2 shows a close-up of the cavity-tuner system. We remind briefly that the slow tuning action is provided by the action of the motor on the leverage arm, which imposes a rotation of the central tuner ring that is transformed, by the blade deformation, in a longitudinal cavity elongation. The fast action is provided by the piezo stacks, with are in series with the force transferred from the tuner to the cavity.

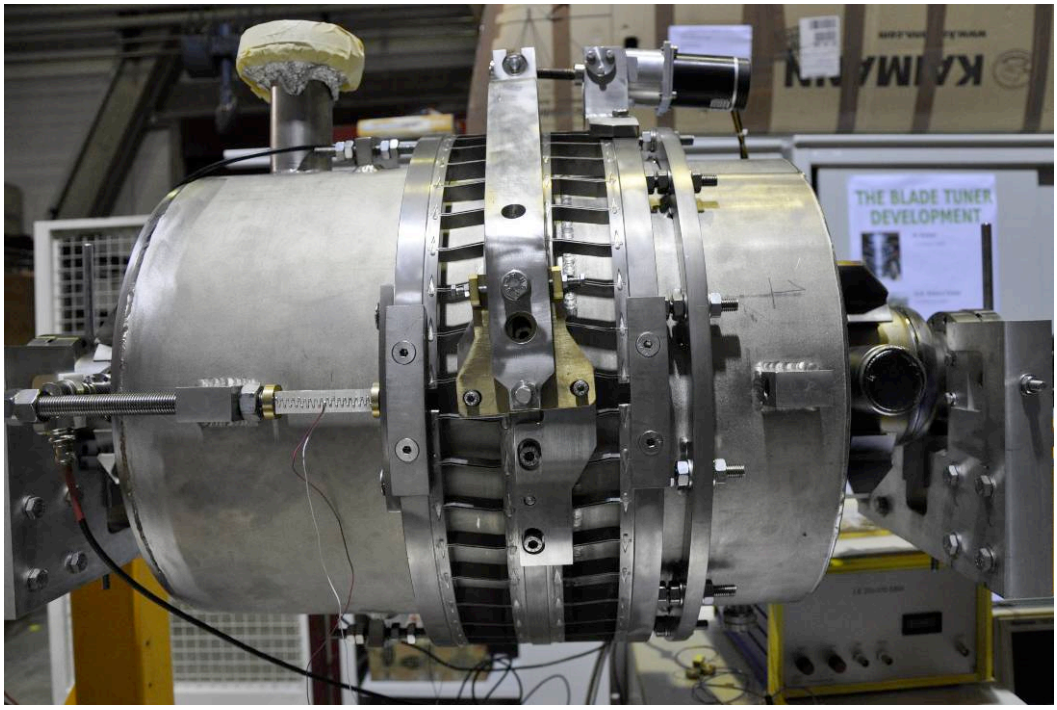

Figure 1.2: Close-up of the cavity and tuner system.

1.4. RESULTS

1.4.1. Cavity Elastic Behavior And Frequency Sensitivity

The cavity elastic coefficient and frequency sensitivity against length variation has been reported in Ref. 1.2, as obtained by mechanical and coupled RF simulations (using Slater perturbation analysis on the nominal geometry), and is reported in Table 1.1.

Table1.1: Cavity stiffness and frequency sensitivity coefficient.

Parameter	Units	Computed	Experimental
Kcav	kN/mm	1.25	1.98±0.04
df/dz	kHz/mm	353	363±13

In order to derive the experimental values reported in Table 1.1, two calibrated load cells have been inserted along the load path from the tuner to the cavity, in order to measure the force exerted on the tuner by the cavity. The flange-to-flange cavity length has then been measured by means of highly sensitive dial gauges with micrometric resolution. The experimental values, with its error, have been obtained by a series of repetitive measurement under the same conditions. During the tuner movement and the measurement of the force the cavity frequency was monitored with the VNA, to derive the cavity frequency sensitivity to elongation.

Figure 1.3 shows the Force measurement data from three tuner cycles, and Figure 1.4 the frequency behaviour.

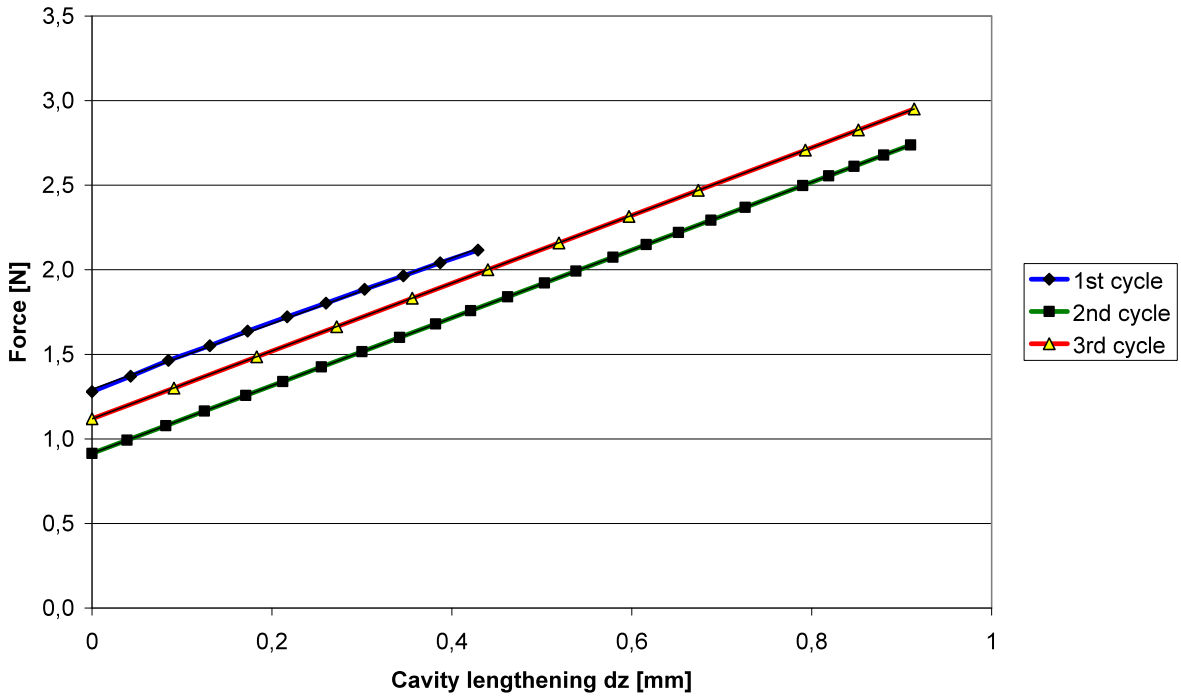

Figure 1.3: Measurement of the tuning force exerted by the tuner on the cavity vs the flange-to-flange cavity lengthening for three different tuning cycles.

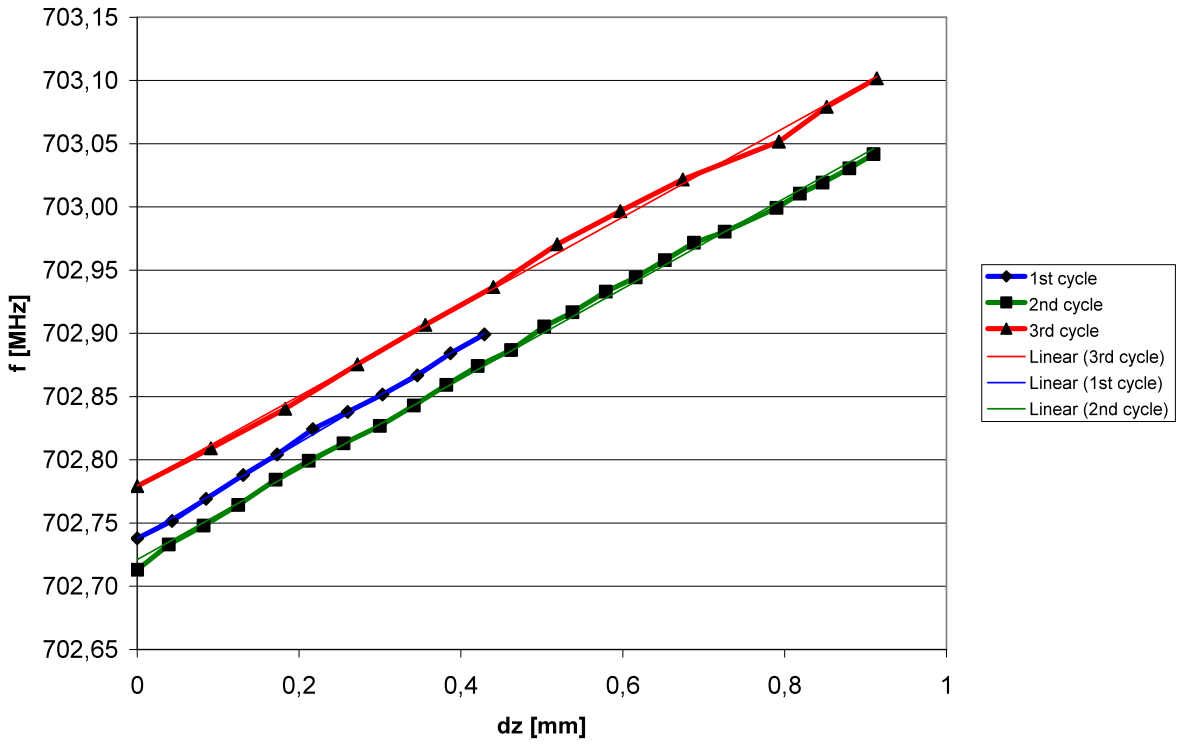

Figure 1.4: Cavity frequency behaviour for the three cycles displayed in Figure 1.3.

Data presented in Table 1.1 shows a very good agreement with the cavity design data presented in Ref. 1.2. The higher cavity stiffness observed during the measurement with respect to the estimations can be safely accounted with the stress stiffening induced in the material by the field flatness operations and with the uncertainties in the material data used for the mechanical analyses.

1.4.2. Slow tuning range

The tuner has been designed to provide a 400 kHz total frequency range at the cavity. This is obtained transferring the maximum tuner elongation of 1.3 mm to the cavity, with a good mechanical efficiency of 92%. The resulting nominal cavity elongation is 1.2 mm.

The ability to provide the complete tuning range relies on the correct positioning of the leverage arm, which is obtained by securing “in-place” the adjustable parts supporting the central ring pivotal points with an interference pin. This “in-place” pinning operation was performed with an incorrect positioning resulting in a somewhat reduced tuning range for the cavity Z502 used for the SLHC activities. For sake of comparison Figure 1.5 shows the Z502 lever arm positioning compared to the correct one as performed on the sister cavity Z501. In order to recover the nominal tuning range a new set of adjustable parts need to be fabricated.

Figure 1.6 shows the measurement of the cavity frequency (red curve, axis on the right) and the cavity elongation (blue curve, axis on the left), in a complete cycle of 23 turns of the motor shaft. The total tuning range is 330 kHz, corresponding of a cavity lengthening of approximately 0.9 mm, limited by the travel of the leverage arm. By reworking the adjustable parts the full leverage travel could be recovered, restoring the nominal tuning range of about 400 kHz. The slight hysteresis appearing in the cavity elongation, which is not seen on the frequency curve, is due to the limited accuracy in the measure of the flange positions.

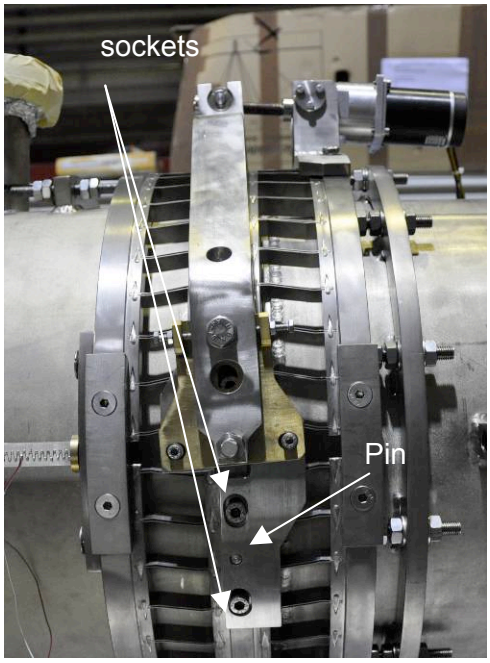

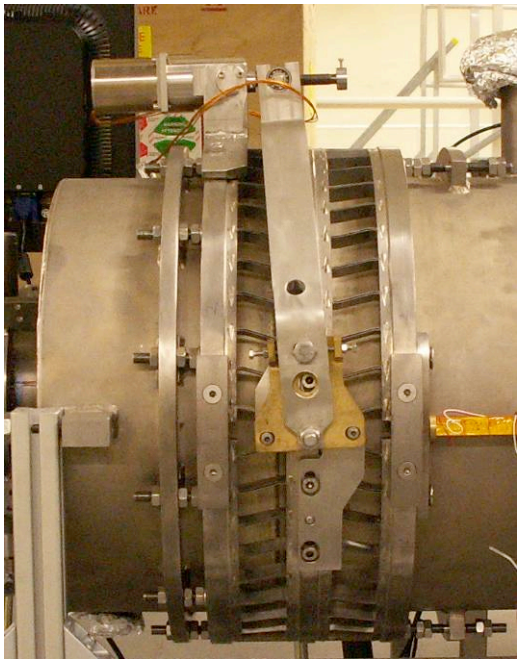

Figure 1.5: Left: The position of the lever arm in cavity Z502 slightly decreases the nominal tuning range due to an incorrect pin positioning, that will be fixed. Right: For comparison, the correct lever arm placement in the sister cavity Z501. (Pictures taken from opposite sides).

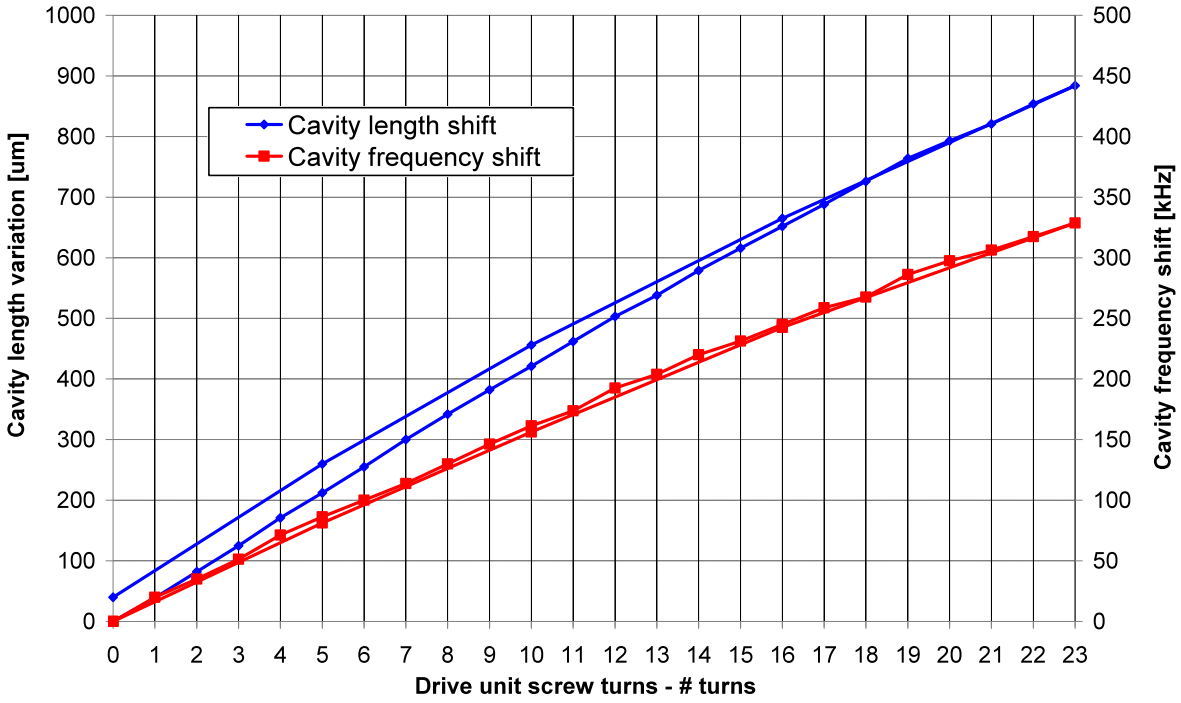

Figure 1.6: Tuning range and cavity elongation.

1.4.3. Static piezo action

With the tuner places roughly midway across the tuning range, a test of the static piezo action was performed, in order to assess the potential corrective action of the chosen piezo stacks (15 x 15 x 70 mm) against dynamic phenomena as Lorentz Force Detuning during pulsed operation or microphonics phenomena. The cavity frequency and flange-to-flange length were monitored after the application of a static voltage to the piezo, in the range from 0 to 200 V. Figure 1.7 shows the results of a single cycle of piezo excitation. The small mechanical hysteresis is compatible with the mechanical piezo characteristics as reported by the manufacturer, and an overall frequency shift of 30 kHz can be obtained at the maximum voltage of 200 V. The choice of this large piezo devices was indeed motivated from the desire to achieve large frequency shifts to counteract the somewhat poor behaviour of the RF structures under pulsed conditions.

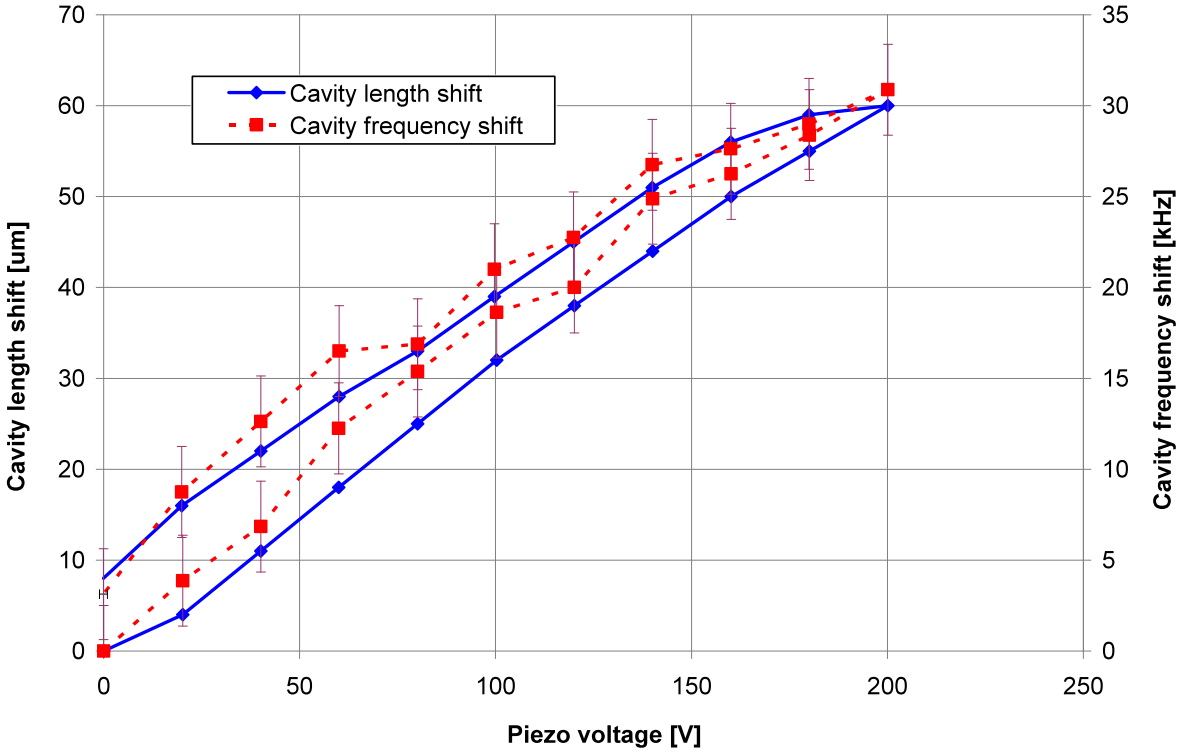

Figure 1.7: Frequency shift and elongation of the cavity under static piezo excitation.

1.4.4. Considerations on Piezo Dynamic Behavior

The piezo stacks have been driven in quasi-static conditions at 1 Hz, with a 50 V peak to peak voltage in order to make an educated guess of the dynamic behaviour of the system. Figure 1.8 shows the cavity RF phase recorded by the VNA, modulated by the pulsed piezo action at 1 Hz. The 5° peak to peak induced phase variations correspond to a frequency variation of approximately 9 kHz. With the present setup we could not test real dynamic conditions at excitation frequencies greater than 1 Hz. This results, however, gives us great confidence for the capability of controlling LFD phenomena at the moderate gradients of approximately 10 MV/m foreseen for these structures, even for LFD coefficients in the range of 10 Hz/(MV/m^2) or more.

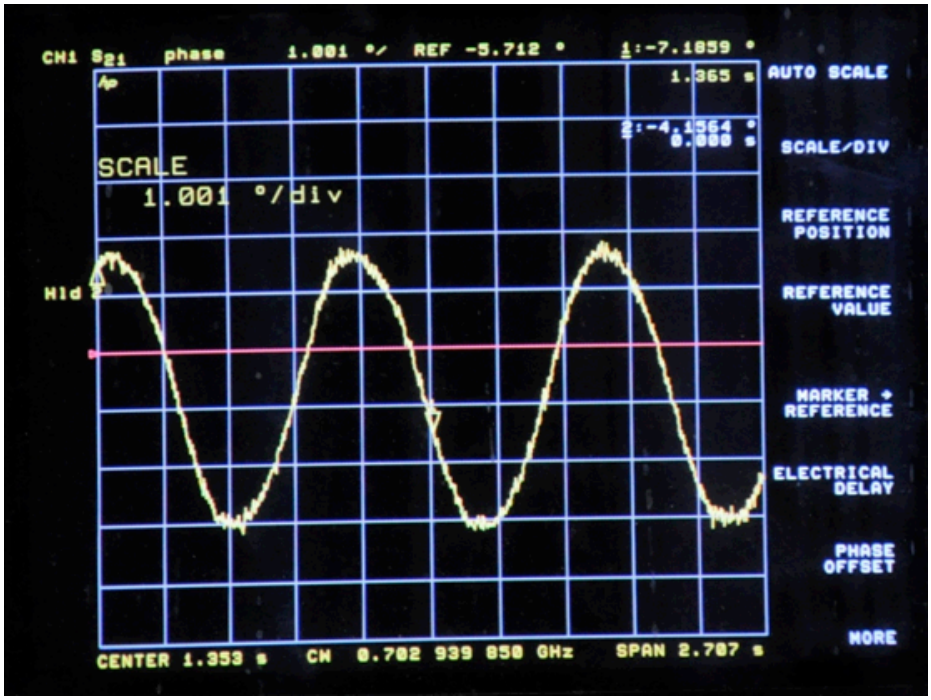

Figure 1.8: RF cavity phase variations induced by a 50 V piezo excitation at 1 Hz.

1.4.5. Pressure Tests

In order to characterize the system in view of the forthcoming tests at CRYHOLAB in Saclay, it was decided to monitor the cavity frequency as a function of the pressure of the Helium bath. To reproduce a situation similar to the future conditions in CRYHOLAB, and since the inner volume of the cavity during this test is at atmospheric pressure, the helium tank volume has been pressurized with nitrogen up to 2 bar of absolute pressure (thus 1 bar relative pressure from the outer cavity surface). During the test both the cavity flange-to-flange distance and the RF frequency have been monitored, in order to derive the cavity sensitivity to the external pressure and an estimate of the stiffening provided by the tuner system to constrain the cavity longitudinally. The latter is an important parameter in order to assess the behaviour of the cavity system under Lorentz Force Detuning.

Figure 1.9 shows the setup of the pressure test. A pressure gauge has been used to determine the tank pressure conditions, dial gauges have been used to determine the cavity flange-to-flange length increase. A pressure limiting valve has been set to about 1 bar on the nitrogen line in order to prevent possible damage of the cavity during testing.

Figure 1.10 shows the behaviour of the cavity frequency against pressure condition in the tank, during a cycle from atmospheric pressure to 1 bar relative pressure and back. The overall cavity sensitivity to the pressure condition in the Helium tank is 321 kHz/bar.

The contribution to the cavity frequency shift is composed of two terms. One is related to the elongation of the cavity due to pressure acting on the end dishes of the cavity tank. The only constraint opposing to this lengthening is the combined stiffness of the cavity and tuner system. Thus, the analysis of the cavity lengthening provides an estimate of the external stiffness provided by the tuner to the cavity itself. The second contribution is the change in the cavity shape due to the pressure forces that would be experienced also in the infinitely constrained case.

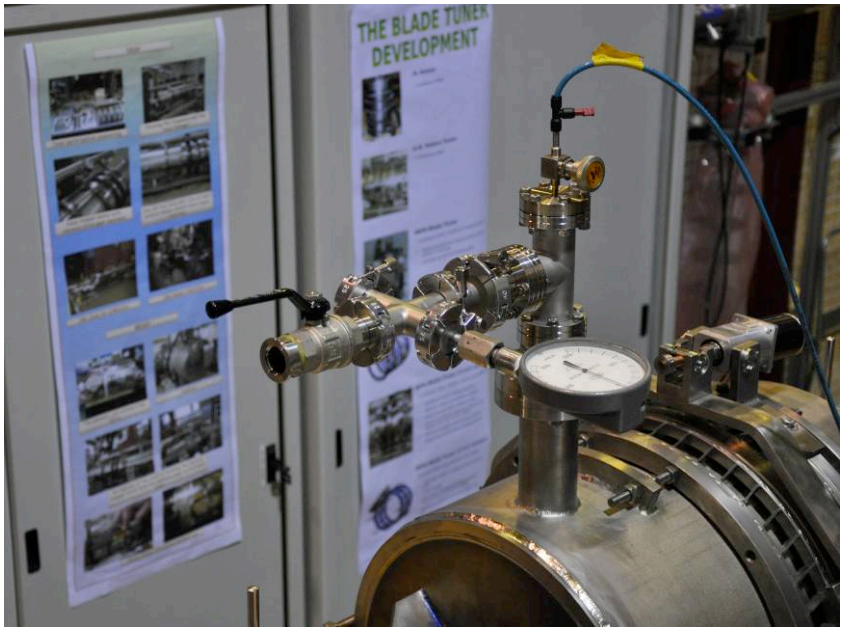

Figure 1.9: Setup of the pressure test.

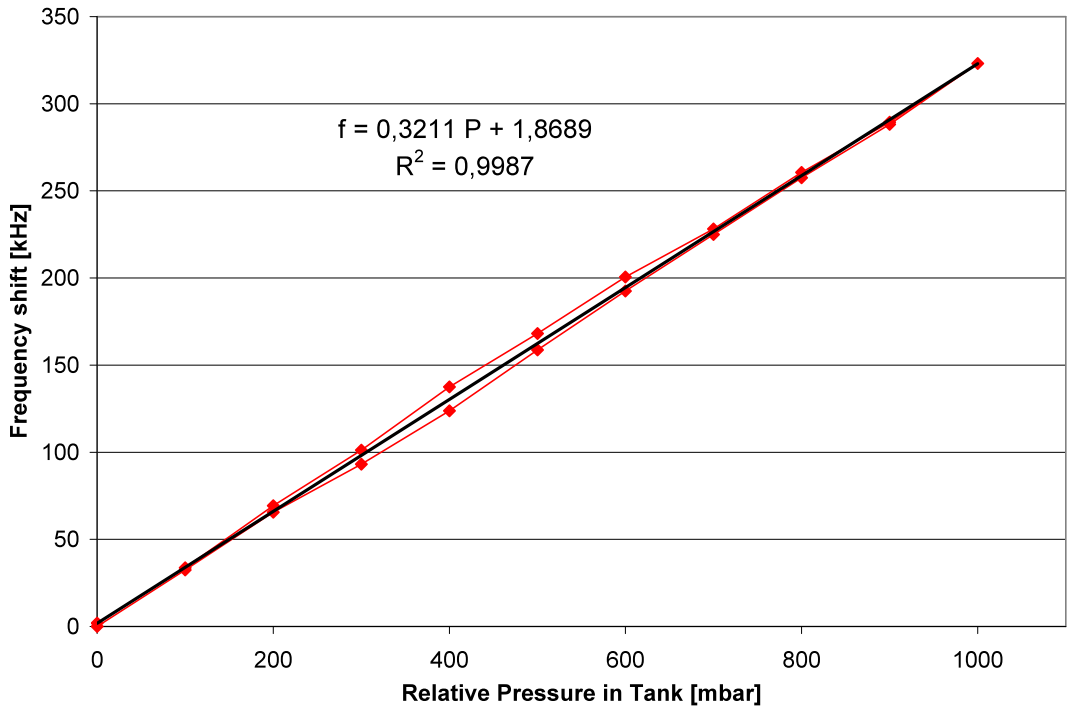

Figure 1.10: Frequency variation of the unconstrained cavity as a function of the pressure condition in the Helium tank.

The pressure sensitivity for the infinitely constrained case has been evaluated in Ref. 1.2, coupling the structural pressure load to a Slater perturbation analysis to obtain the frequency deviation. The estimation for this contribution is 85 Hz/mbar for a uniform cavity thickness and 104 Hz/mbar if considering the thickness reduction in the real cavity performed for the equatorial welds.

The behaviour of the cavity lengthening against the relative pressure in the tank is shown in Figure 1.11. The overall coefficient is 0.558 mm/mbar of applied pressure.

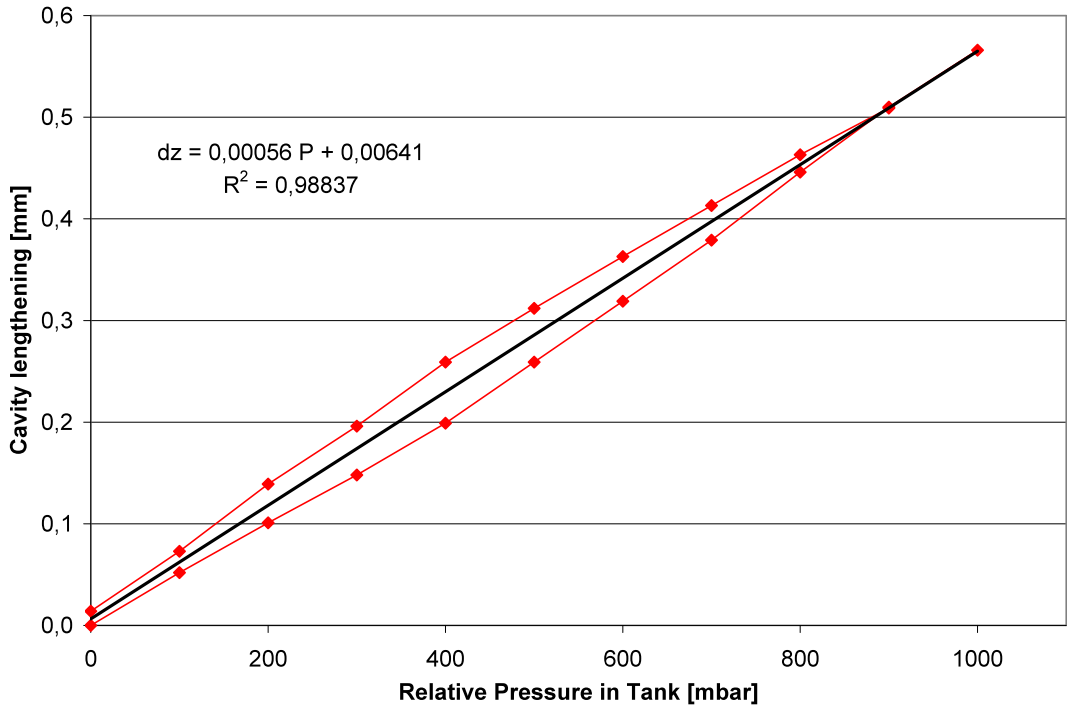

Figure 1.11: Lengthening of the unconstrained cavity as a function of the pressure condition in the Helium tank.

The analysis of the curves in Figure 1.10 and 1.11, along with the characterization of the cavity stiffness performed in the previous paragraphs allows to determine the experimental value of the pressure sensitivity of the infinitely constrained case (which evaluates to 118 Hz/mbar, within 15% of the ANSYS/Slater prediction). Moreover, from the lengthening data we have derived that the “external” stiffness provided by the tuning system to the cavity in order to constrain its extension is approximately 14 kN/mm, a value that exceeds the minimal requirement of 3 kN/mm needed to allow safe margin in the LFD control.

1.5. CONCLUSIONS

We have reported here the characterization of the INFN cavity/tuning system at warm condition, which is important in order to gain the relevant information on the device prior to the cold tests in CRYHOLAB, which are scheduled during 2010.

1.6. REFERENCES

[1.1] A.Bosotti et al., CARE Note-2005-001-HIPPI

[1.2] P.Pierini et al., CARE Note-2006-003-HIPPI

[1.3] J. Plouin, CARE-Report-08-055

2. PART B

2.1. EXECUTIVE SUMMARY

We report here the activities for the characterization of the low beta 5-cell superconducting elliptical cavity designed by CEA-Saclay at cryogenic temperature performed in the horizontal test cryostat CRYHOLAB installed at CEA Saclay.

2.2. INTRODUCTION

During the CARE-HIPPI joint research activity of the FP6 program [2.1], low beta superconducting (SC) elliptical cavities operating at 704 MHz have been designed and tested. Based on earlier R&D programs, mainly on Accelerator Driven Systems (ADS) like ASH [2.2] and TRASCO [2.3], two cavity designs were pursued in INFN Milano and CEA-Saclay, in order to study the possibility of accelerating protons with elliptical superconducting multi-cell cavities in the energy range of 80 to 200 MeV. The beta (ratio of particle over light velocity) of these cavities is 0.5. After optimization of the electromagnetic design of the cavity, the cells have a flat aspect ratio, which represents a challenge for mechanical stability and stable frequency operation in a realistic accelerator environment. Compared to beta=1 SC cavities employed on electron linear accelerators, their frequency is more sensitive to Helium pressure variation, and to electromagnetic pressure (Lorentz detuning). In the beginning, these cavities were developed with CW accelerators in mind, were the static Lorentz detuning can be compensated by adjusting the cavity resonant frequency accordingly using a standard mechanical tuner. One goal of the CARE-HIPPI program was to design and test this type of cavity in pulsed mode, which is more demanding, since the cavities are then periodically excited by the Lorentz force so that the mechanical modes of the system have to be taken into account.

To mitigate the Lorentz force detuning (LFD), two ways have been pursued: first, welding rings in the iris region of each cell, at an optimized location to minimize the Lorentz force coefficient KL; second, using a fast piezo tuner able to compensate the residual dynamic detuning which occurs during the RF pulse. The EM characteristics of the INFN and CEA cavities are similar, but the options for the minimizing the LFD are different: the INFN cavity has one series of rings, the CEA cavity has two to further reduce the KL coefficient further [2.4]. For that reason they are mechanically different. Although running in pulsed mode, the cavities are usually compared with respect to their LFD static coefficient, due to incomplete information on their dynamical behavior at the design stage. The uncertainty on so many parameters such as the quality factor of the large number of mechanical modes prevents to derive a realistic comparison of the dynamical detuning of two different designs. One clear indicator of this fact is the great difference in the RF and mechanical response of the cavity to mechanical excitation before and after it is equipped with its tuner. The latter plays an important role in the system response and is even more difficult to model numerically.

The experimental characterization of the dynamical behavior is therefore indispensible in order to get data on the mechanical mode characteristics. Numerical modeling can then predict the behavior of the cavity in realistic operating conditions, and give an insight into the low level RF requirements. One objective of the task 7.2 of SLHC-PP is to explore the potential of driving multiple cavities using one RF power source, and to determine the necessary power overhead and distribution layout. The SPL design does not include such low beta elliptical cavities, but the design of any higher beta section will benefit

from the experimental data and experimental use of the prototype components such as the power coupler and piezo tuner.

2.3. THE BETA 0.5 SACLAY CAVITY

The design parameters of the cavity are recalled in table 2.1:

Frequency [MHz]	704.4
Epk/Eacc	3.36
Bpk/Eacc [mT/(MV/m)]	5.59
r/Q [Ω]	173
G [Ω]	161
Q_0 @ 2K Rs=8 nΩ	$2\ 10^{10}$
Optimal β	0.52
Geometrical β	0.47
Total length [mm]	832

Table 2.1: main cavity parameters

Bare cavity stiffness [kN/mm]	2.25
Tuning sensitivity $\Delta f/\Delta l$ [kHz/mm]	295
K_L @ k_{ext} = 30 kN/mm [Hz/(MV/m)²]	-3.9
Lorentz Δf@ 12 MV/m, k_{ext} =	-560
K_L with fixed ends	-2.7
K_L with free ends	-20.3

Table 2.2 : Mechanical and static coupled RF/mechanical parameters

Static behaviour of the cavity with various boundary conditions have been evaluated using FEM codes. The main cavity simulated parameters including coupled RF/mechanical computation results are shown in table 2.2.

The end cells are identical, and connected to the beam pipe which is 130 mm in diameter. One beam tube supports the power coupler port (left side on fig. 2.1), while the other is equipped with a pickup and is compatible with the installation of the tuning system.

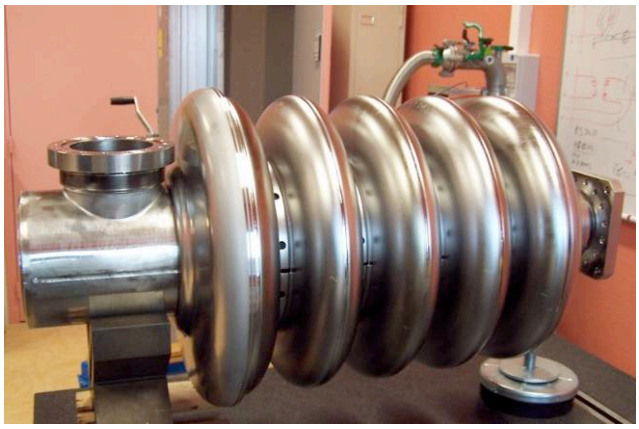

Figure 2.1: The bare Saclay 5-cell 700 MHz elliptical cavity.

The coupled mechanical/RF parameters of main interest are

- The tuning sensitivity $\Delta f/\Delta L$, easiest to measure, independent of temperature and boundary conditions.
- the pressure sensitivity $\Delta f/\Delta P$, which can be measured in various setups:
    - at room temperature with the helium tank, using a mechanical system to keep the cavity length constant, which has a given finite stiffness kext
    - in a vertical cryostat with or without He tank, fully immersed in liquid He, also using an external stiffening system to keep the cavity length constant, varying the He pressure if possible, from 1000 mbar down to whatever pressure the He pumping system is capable of, in our case 5 mbar. The cavity is under vacuum so the He pressure is also applied on the closing flanges.
    - In a horizontal cryostat with He tank. Several external stiffening systems have been used in our case, one of them being the actual tuning system. The He pressure can also be varied between 1200 and several mbars. The load case is different from what is obtained in the vertical cryostat since no pressure is applied on the cavity closing flanges. Another change with respect to the vertical cryostat test conditions lies in the outwards pressure the He tank experiences on its outer shell.
- The static Lorentz coefficient KL. Its measurement requires reaching high accelerating field values with CW RF power. It can only be measured in the superconducting state of the cavity. It is generally measured when the cavity is equipped with a weakly coupled field probe pick-up and a close-to-critically coupled forward antenna. It can be measured both in vertical and horizontal cryostat, but again, the results will depend on the external stiffness Kext of the external mechanical system keeping the cavity length constant. Measuring the static KL when the power coupler is assembled on the cavity is still possible but requires a high power CW RF source of several tens of kW for a typical Qext of 10^6.

The KL coefficient is also dependent on the effective thickness of the cavity walls as can be seen in figure 2.2. The design thickness was 4 mm, but this value could not be maintained due to the manufacturing process and chemical processing. An average of 3.3 mm is more representative of the final test conditions. We will refer to this thickness as the effective thickness.

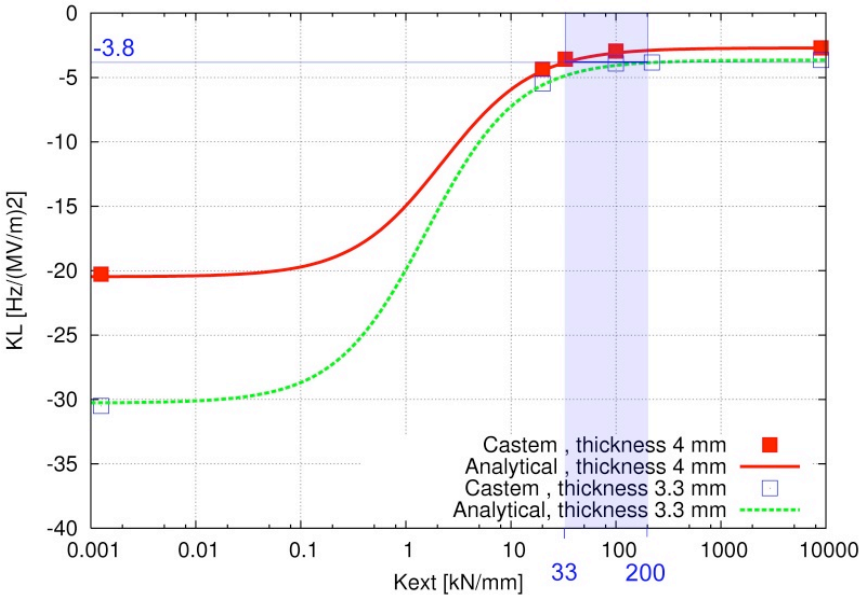

Figure 2.2 : dependence of KL on the external stiffness Kext

The dependence of KL on the external thickness was the basis to set a goal on the external stiffness, which results from the series combination of the He tank and tuner. From experience gathered on other similar tuning systems we noticed that obtaining a reproducible stiffness above 50 kN/mm was not realistic for the tuner itself. The series combination of a 100 kN/mm He tank and a 50 kN/mm tuning system is a good compromise to obtain a global external stiffness of 33 kN/mm, keeping the effective KL modulus below 4 Hz/(MV/m)^2.

2.4. PRELIMINARY MEASUREMENTS ON THE CAVITY

2.4.1. Room temperature measurements

The cavity wall design thickness was 4 mm with a reduction at the equatorial welds, but due to the fabrication processes, the final thickness was reduced and not uniform, with an average value of 3.3 mm [2.4]. The mechanical parameters related to cavity RF performance have been measured first at room temperature on the cavity tuning bench before the He tank welding. The tuning sensitivity has been measured to be 290 kHz/mm. After the welding of the helium tank, just before the test in the vertical cryostat, a piezo actuator was installed between the stiffener and the helium tank in order to excite the longitudinal mechanical modes of the cavity. The measurement of the piezo drive voltage-to-cavity detuning was carried out using harmonic excitation. The detuning signal is generated by a phase demodulation system pictured in fig. 2.3. A lock-in amplifier coupled to a PC records the detuning. This measurement method has the advantage of a high spectral resolution and low noise permitted by the synchronous detection, at the expense of acquisition time.

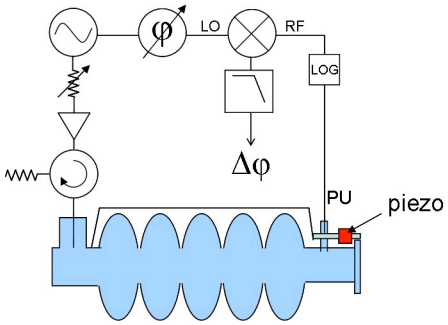

Figure 2.3: phase demodulation system

The resulting piezo voltage-to-cavity detuning transfer function displays mainly longitudinal mechanical modes of the cavity (fig. 2.4):

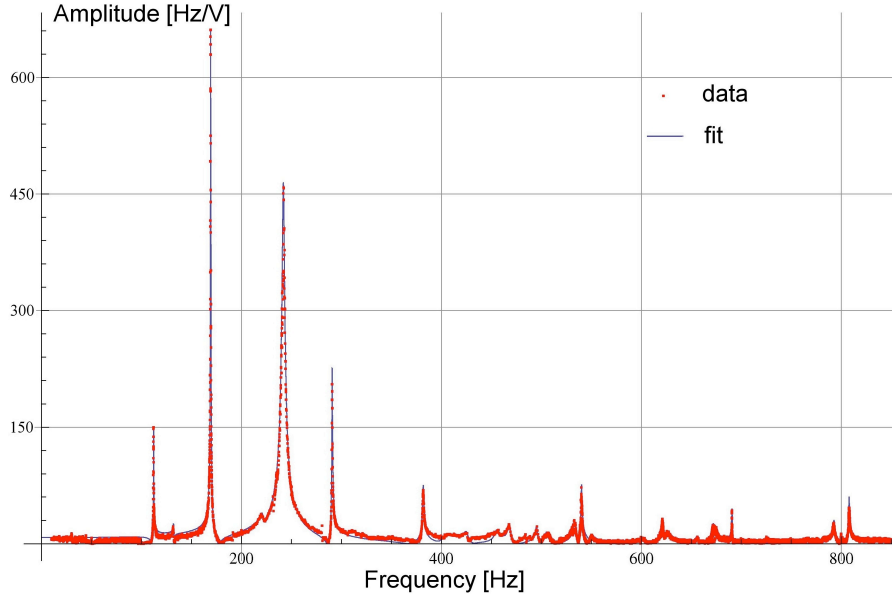

Figure 2.4: Amplitude of the bare cavity piezo voltage to detuning transfer function at 300K.

The measured frequencies of the first main longitudinal modes can be compared to calculations which have been carried out with the CASTEM FEM mechanical code, using a 2D axi-symmetrical model with a solid mesh (table 2.3). The agreement between both sets of data is satisfactory, given the thickness variation among the cells, which has not been modelled numerically. Instead an average value of 3.3 mm has been taken as the constant thickness of the model, with the exception of the welds for which the thickness was known from the manufacturing process.

Frequency (simulation) [Hz]	Frequency (meas.) [Hz]	Q_m (meas.)
95	112	400
184	169	500
240	242	90
300	291	500

388	382	300
477	468	195
549	540	500
605	601	100
628	621	350
665	672	300
690	691	1000

Table 2.3: comparison of computed and measured longitudinal mechanical modes

Very high mechanical quality factors (Q_m) have been measured, but this cavity setup is not representative of the operational conditions in a cryomodule. In operation, the cavity is mechanically coupled to supports, tuning system, power coupler, cryogenic piping, which can provide damping for the cavity modes and bring their own mechanical modes making it a more complex system.

2.4.2. Vertical cryostat CW measurements

The characterisation of the cavity in the vertical cryostat was first done on the bare resonator [2.4]. Then a second series of tests was carried out after welding the He tank to the cavity. In order to maintain the cavity frequency and mechanical stability during pumping and cryogenic tests, a stiffener (upper part of fig.2.5) was installed at the final location of the tuning system which was not yet available for the vertical tests.

Figure 2.5: cavity setup with He tank and stiffener for vertical cryostat measurements.

This stiffener and the actual tuning system were made comparable as far as their stiffness is concerned, in order to obtain first realistic results on the effective KL of the complete system.

The main results from vertical tests are the Q=f(E) characteristic curve of the cavity (fig. 2.6) measured at 1.8 K, in CW mode.

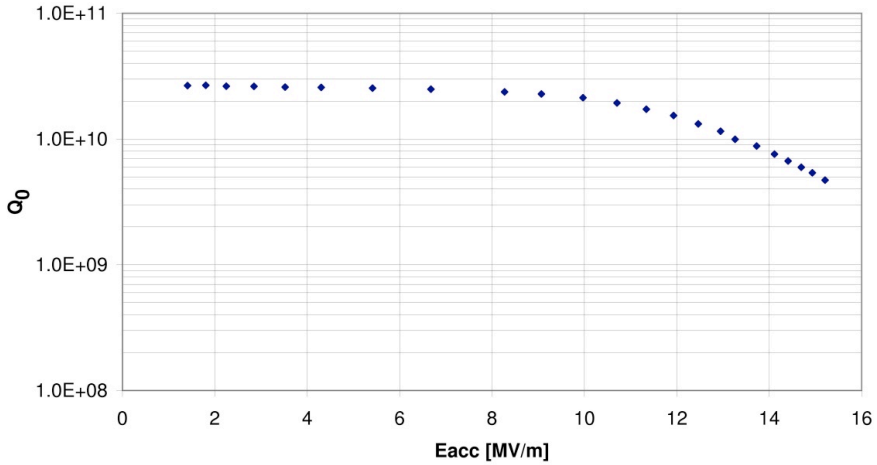

Figure 2.6 : Q=f(E) measurement in vertical cryostat.

The Lorentz detuning coefficient of this cavity configuration has been measured. A value of KL=-3.8 Hz/(MV/m)^2 can be derived from the experimental data (fig. 2.7):

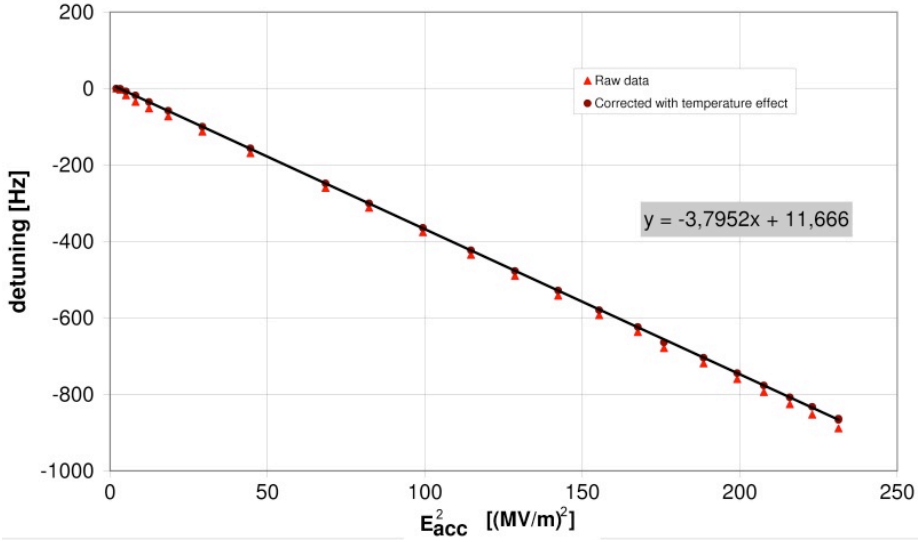

Figure 2.7: Lorentz detuning measurement

More details on these measurements can be found in [2.5].

2.4.3. 4.3 Horizontal test in CW

The same setup was installed in the CryHoLab [2.6] horizontal test cryostat. The main purpose of this test was to test the magnetic shielding designed specifically for this cavity [2.7] and look for differences in thermal behaviour of the cavity under cooling conditions different than in the vertical cryostat. Nothing was changed for the coupler end-group since it is enclosed in the He tank, but the tuner side end-group is now under vacuum. Field

emission was observed during the tests, for Eacc above 8 MV/m. It was conditioned, leading to the best measurement shown on figure 2.8 (blue dots).

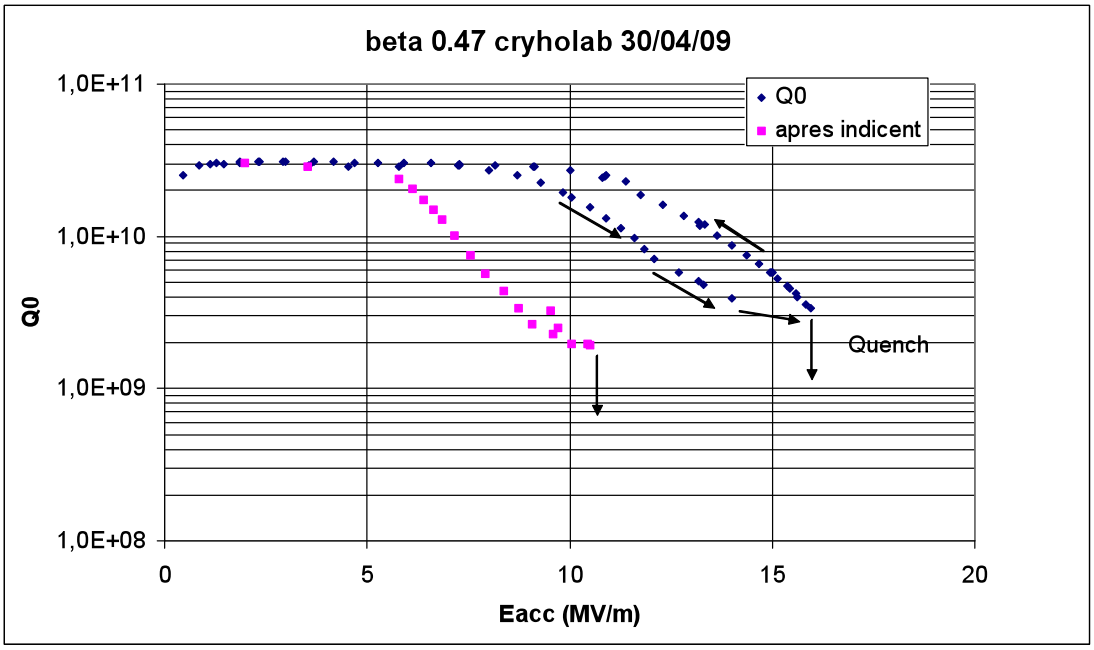

Figure 2.8 : Q=f(E) curves in Cryholab at 1.8K

The maximum field obtained was 16.5 MV/m. During a measurement on the $4\pi/5$ mode of the fundamental passband, field emission resumed and could not be processed, heavily plaguing the cavity performances (magenta dots on fig. 2.8). This lead us to carry out a new processing on the cavity before full tests with the power coupler.

2.5. THE FAST PIEZO TUNER

Previous tuner designs for elliptical cavities based on the SOLEIL type have been prototyped and tested at Saclay. The tuner developed in the FP6 CARE-SRF programme was the first version with a piezo actuator to be designed on this basis for a 9-cell TTF-Tesla 1.3 GHz cavity (Saclay II). Since the Saclay II tuning system showed good performance, its major design options have been retained for the 704 MHz cavity tuner (fig. 2.9):

- A symmetric slow tuning part with lever arms converting the transverse action of a screw into a longitudinal displacement through eccentric rods.
- cryogenic operation of the stepper motor and gear box in insulation vacuum
- gear box ratio around 100 in order to achieve high resolution and torque
- a fast tuning mechanism consisting of a piezo frame on one side of the tuner only. This means that the piezo stroke is not fully converted into cavity lengthening.
- Noliac 30 mm low voltage piezo stacks, 10x10mm section

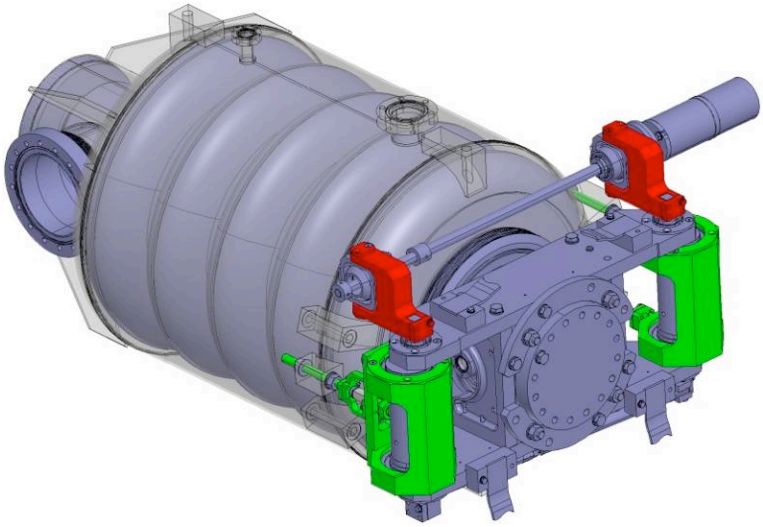

Figure 2.9: CAD model of the 704 MHz tuner

However, the mechanical system has been redesigned to simplify the installation on the cavity, by just sliding the fully assembled tuner in place. The piezo support design has been upgraded for the 704 MHz tuner, the main design changes are listed below:

- it contains one piezo only (fig. 2.10).
- it comprises a rigid frame and one preload screw only, so it is much simpler
- it is 10 times stiffer than the cavity in order to maintain the piezo preload independent of the cavity tuning. In the Saclay II design the piezo load was only due to the reaction force of the cavity when elongated. The cavity frequency had first to be raised by several hundreds of kHz with the slow tuning mechanism in order to operate the piezo tuner with a correct preload.

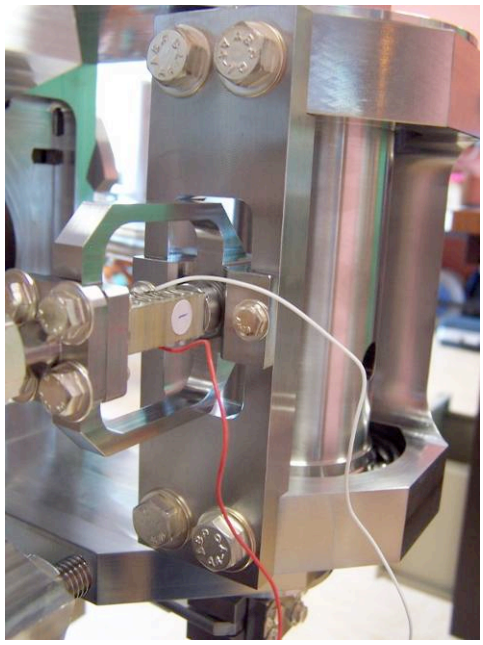

Figure 2.10: piezo support

The tuning system is attached to the He tank at three points, one on the piezo side, and two on the opposite side. The main beams of the tuner are fixed to the cavity flange. The tuner has been installed on the tuner pneumatic jack bench in order to measure its stiffness. The three tuner supports are connected to the jack body. A stainless steel thick disk fixed on the jack stem simulates the cavity flange. Its displacement is measured with a dial gauge for a given calibrated force. The direction of the force is chosen to reproduce the shrinkage of the cavity subjected to the radiation pressure, corresponding to a compression force on the tuning system. The measured relative displacement of the flange with respect to the jack body is 0.2 mm for a 7000 N force, which leads to a stiffness of 35 kN/mm.

2.6. PREPARATION AND INSTALLATION OF THE FULLY EQUIPPED CAVITY IN CRYHOLAB

2.6.1. 6.1 Coupler and cavity assembly

A light chemical etching of the cavity with a standard FNP mixture was carried out prior to high pressure water rinsing to refresh the cavity surface after observation of a strong field emission during the previous tests. The power couplers had already been processed up to 1.2 MW in travelling wave mode in the first quarter of 2009. The couplers and coupling box were filled with dry nitrogen and stored for several month. Just before entering the clean room, the air side of the windows is protected, the assembly cleaned and brought into the clean room of the Saclay/Orme des Merisiers site. One of the couplers is then transferred from the coupling box to the cavity in the class 10 area of the clean room. The assembly sequence is shown on the next figures. Supporting rails are installed in the laminar flow area. The cavity left drying, then it is rotated using a robot arm and installed on its support (fig. 2.11a). The same robot arm is used to lift one of the couplers which is blown with clean nitrogen (fig. 2.11b). The cavity is then sled under the coupler, and the connection between the two is made.

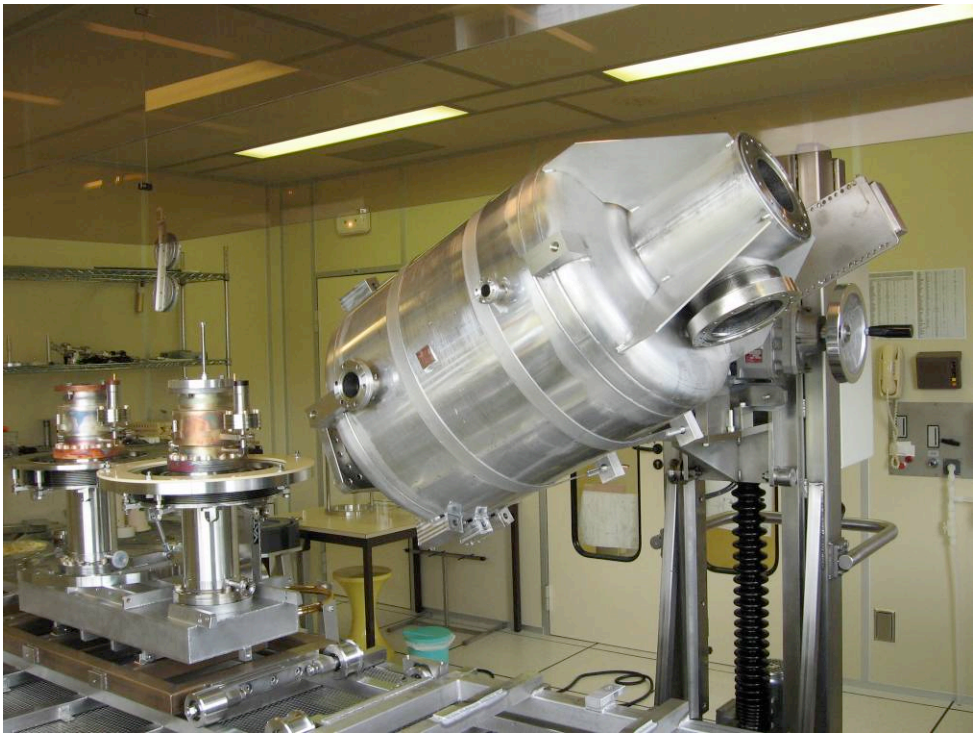

Figure 2.11a: Cavity rotation under laminar flow

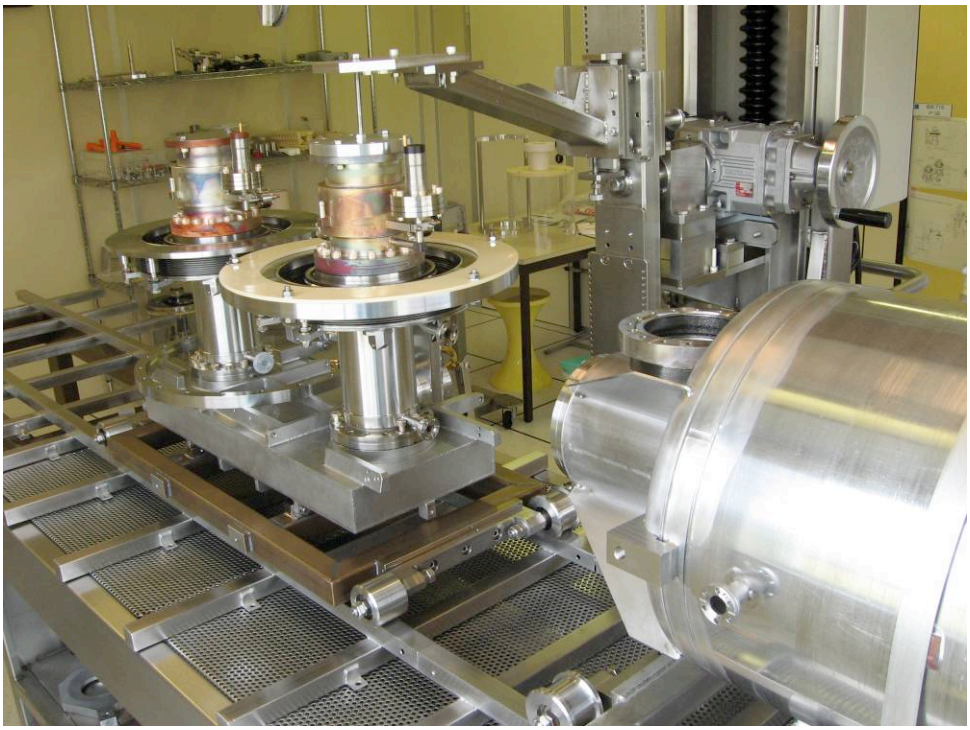

Figure 2.11b : Lifting the coupler

Figure 2.11c: Assembly completed.

The reason for assembling the coupler from above in upright position is to make the tools simpler and compatible with the existing laminar flow dimensional constraints. It is not the most favorable case for cleanness, because the coupler generates a perturbation of the flow above the cavity. In this case the contamination is mostly expected from the coupler flange rather than from the coupler inner surfaces, but the flange can be clean accordingly beforehand.

For this cavity the vacuum leak check cannot be performed in the clean room without using heavy stiffening tools, so it is delayed until after the tuning system installation.

2.6.2. Cryholab test configuration

In the final configuration, the coupler and the tuning system are in horizontal position (fig. 2.12).

Figure 2.12: Frequency check after coupler and tuning system assembly

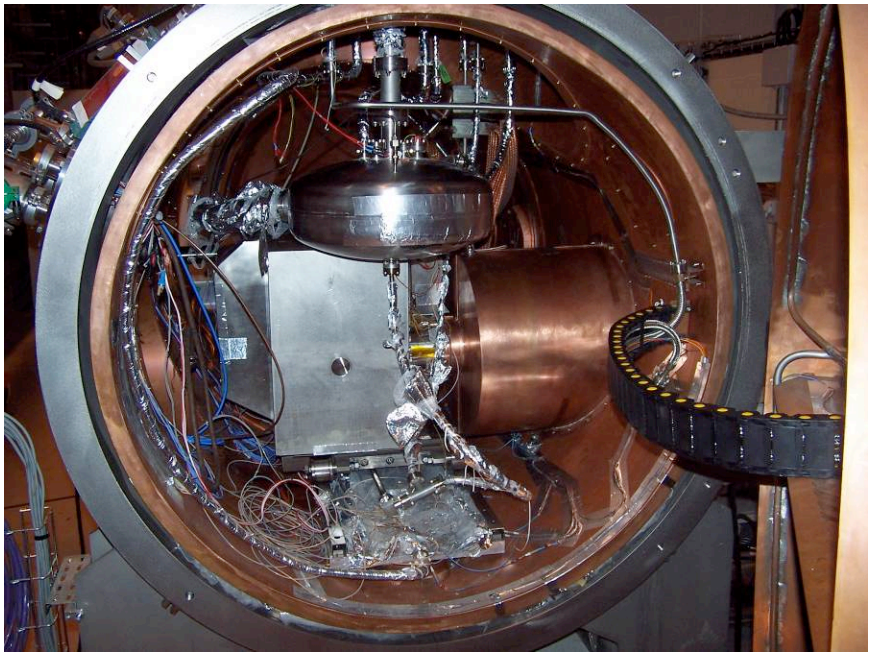

Figure 2.13: the fully equipped cavity in Cryholab.

The horizontal test set up also includes the super-insulation blanket and the magnetic shielding enclosing the whole cavity. In the Cryholab, the fully equipped cavity can be rolled into place. This explains the off-center positioning of the cavity (fig. 2.13). The air side of the coupler connection is shown in figures 2.14 a and b.

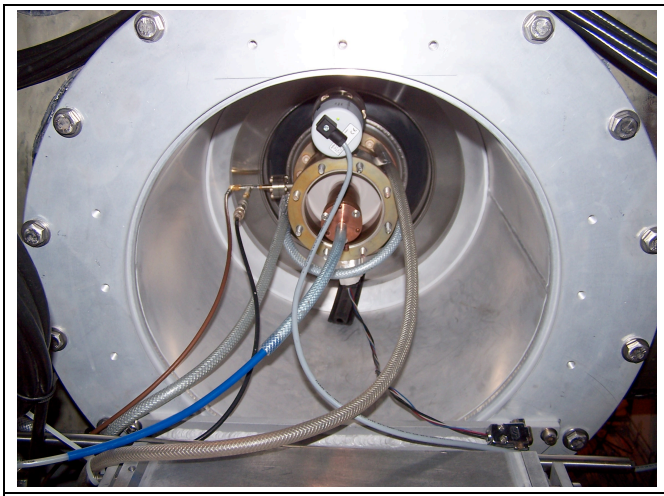

Figure 2.14a: connection between the coupler and Cryholab

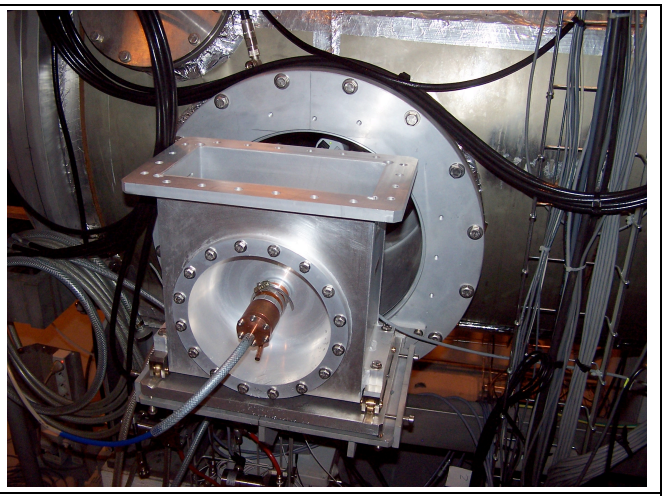

Figure 2.14b: Doorknob transition aligned on its table

The mechanical configuration for the tests is not the same as in a linac cryomodule where it is of high importance to maintain the cavity alignment during thermal cycles. Instead, it is the following:

- The bellow connecting the coupler flange and the RF window provides flexibility during the assembly. Once all the parts forming the vacuum vessel seen on fig. 2.13a are connected, the bellow is locked in position using adjustment screws. This is to counteract the pressure force on the coupler flange due to the insulation vacuum. As a consequence, the power coupler flange is a fixed point.
- The cavity can move sideways with respect to the supporting rails during cooldown to withstand the shrinkage of the power coupler outer conductor.
- The longitudinal position of the cavity is fixed by the coupler. It is supported by a rolling tray, such that both the tray and the rails can freely shrink underneath at different rates without trouble.

2.7. LOW POWER TESTS IN HORIZONTAL CRYOSTAT

2.7.1. Qext measurements

The theoretical distance between antenna tip and beam axis is 70 mm. The 3D computations with HFSS (fig. 2.15) for this setup indicate a corresponding Qext of 1.65e6.

The measured cavity bandwidth is 380 Hz with the power coupler mounted, which corresponds to a Qext of 1.85e6. This 12% difference between simulation results and measurements can be partially explained by fabrication errors and the uncertainty on the two CF connections assembly:

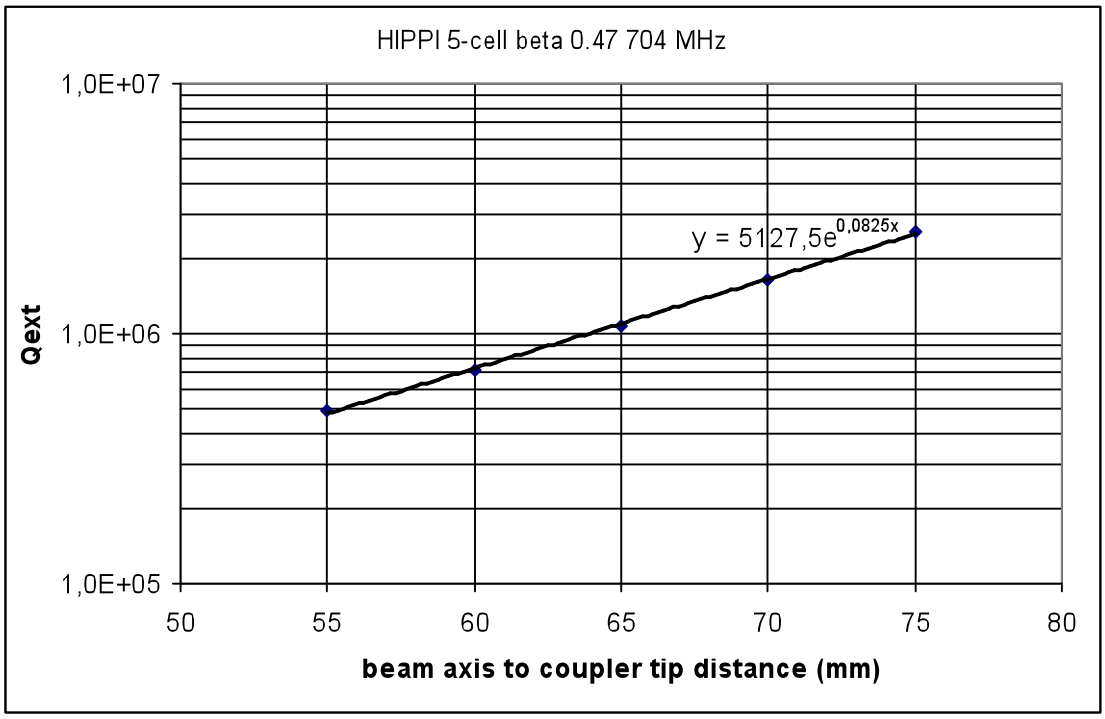

Figure 2.15: HFSS computation of the external Q with respect to the coupler antenna tip position

After the antenna electron beam welding, the manufacturer reported an additional shrinkage of 0.91 mm, due to an extra smoothing pass during the welding process. The theoretical Qext expected taking into account this new antenna length is 1.79e9, which reduces the relative error on the measured Qext to only 3%.

2.7.2. Tuning system characterization

The tuning system is equipped with thermal sensors, which indicate the temperature of the two main beams is around 20 to 25 K after cool-down. The mechanical tuner characteristic curve represents the frequency variation as a function of the number of step sent to the stepper motor. The tuner has only been used in the positive tuning range, corresponding to the direction in which the cavity length is increased and its resonant frequency increases (fig 2.16.)

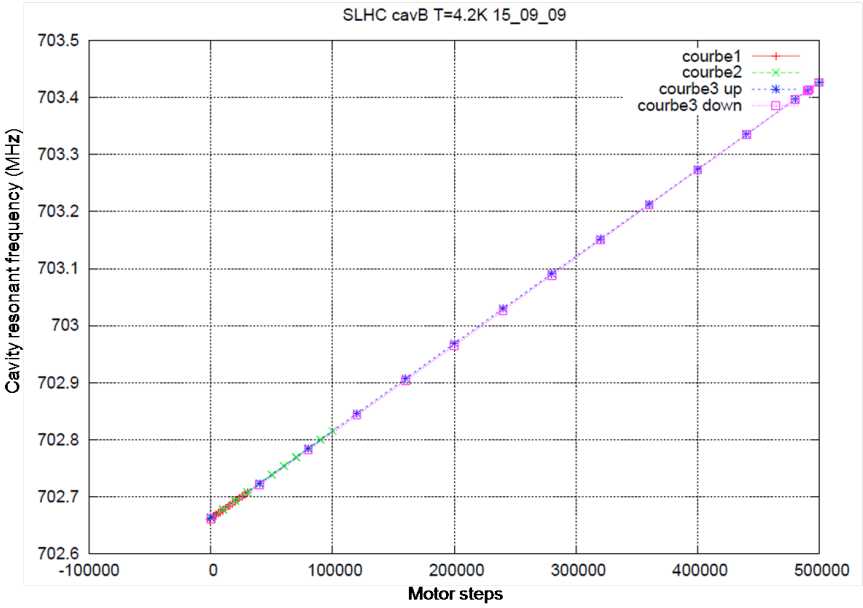

Figure 2.16: motor steps versus cavity detuning measurement

The total positive detuning is 760 kHz with a very good linearity over the whole range. This corresponds to a cavity elongation of 2.5 mm. All the following measurements on this cavity in the Cryholab have been carried out at 703 MHz.

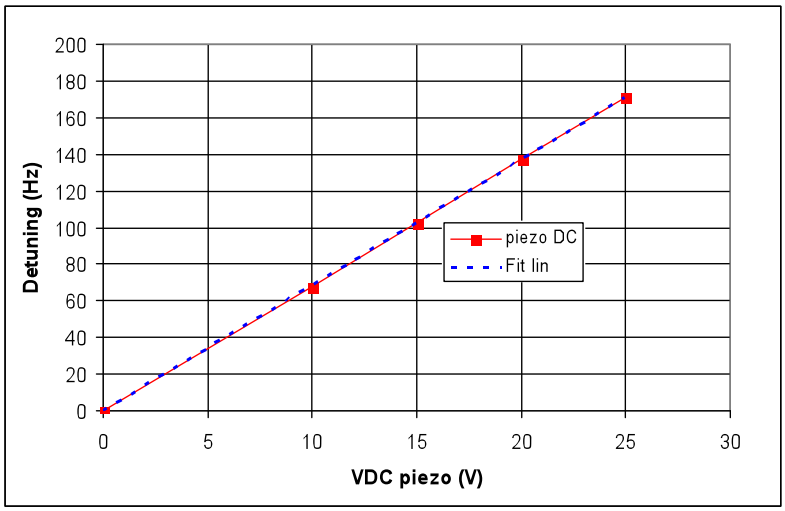

Figure 2.17: fine detuning characteristic of the piezo actuator

The linearity of the piezo action on the cavity detuning has also been measured (fig. 2.17) using a DC voltage. The maximum detuning obtained for a 150 V control voltage on the piezo is 1 kHz.

2.7.3. Piezo to detuning transfer function

Most of the information on cavity modes and how they interact with cavity detuning can be learnt from the piezo to detuning transfer function. The same measurement setup than for room temperature measurements on the bare cavity has been used on the fully equipped cavity at 1.8K, tuned to 703 MHz, but this time, the actuator is the piezo element of the tuning system (fig. 2.18).

Figure 2.18: transfer function measurement and piezo control system (left rack) and stepper control system (right rack) sitting next to the Cryholab shielding.

An example of transfer function measured in the 10 to 800 Hz range is shown on figure 2.19.

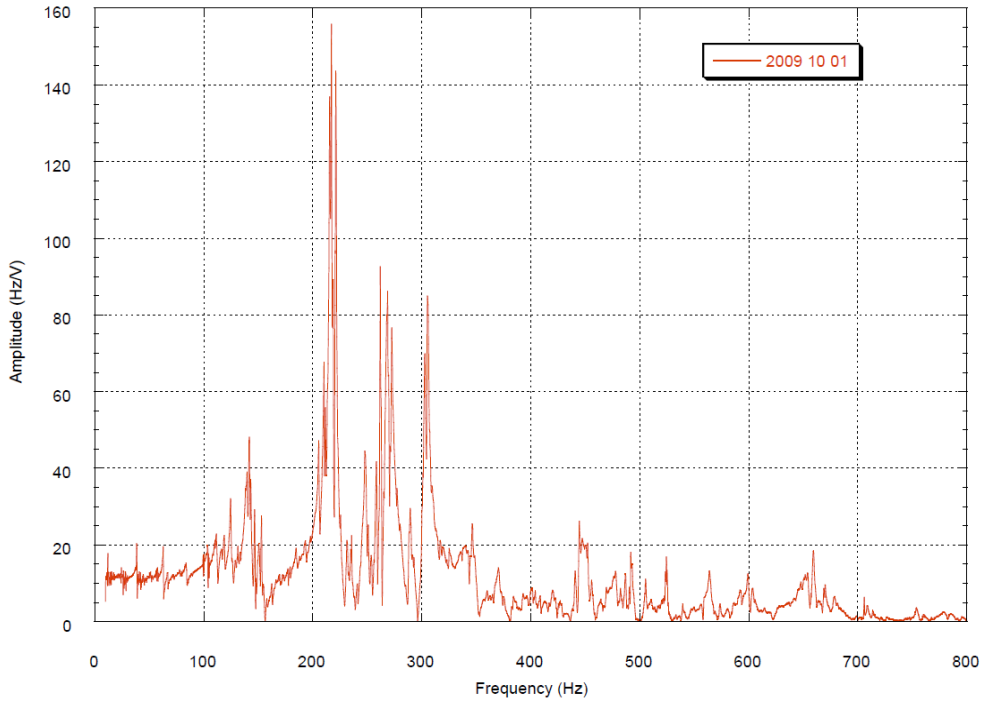

Figure 2.19: piezo voltage-to-cavity detuning transfer function (amplitude)

As expected, the response of the fully equipped cavity in the cryostat is much more complex than what has been measured on the cavity with its helium tank and stiffener tube only due to the large number of mechanical elements being involved. The frequency resolution of this measurement is 0.2 Hz. The modes which display the highest coupling to the cavity detuning are all in the 220-320 Hz range. It is remarkable that none of the modes identified on the cavity and He tank have kept their characteristics, either being shifted in frequency or damped or both. Therefore the identification of the mechanical modes of figure 2.19 using the calculation data of table 2.3 is problematic.

2.8. HIGH POWER TESTS

2.8.1. The pulsed RF power source

The high power RF source has been installed and commissioned at Saclay during the CARE-HIPPI FP6 program [2.8]. It delivers 1 MW, 704 MHz pulses up to 2 ms length and 50 Hz repetition rate. It consists in a 110 kV 2.4 A high voltage power supply (HVPS), a high voltage pulse generator supplying 90 kV pulses to the klystron (fig. 2.20).

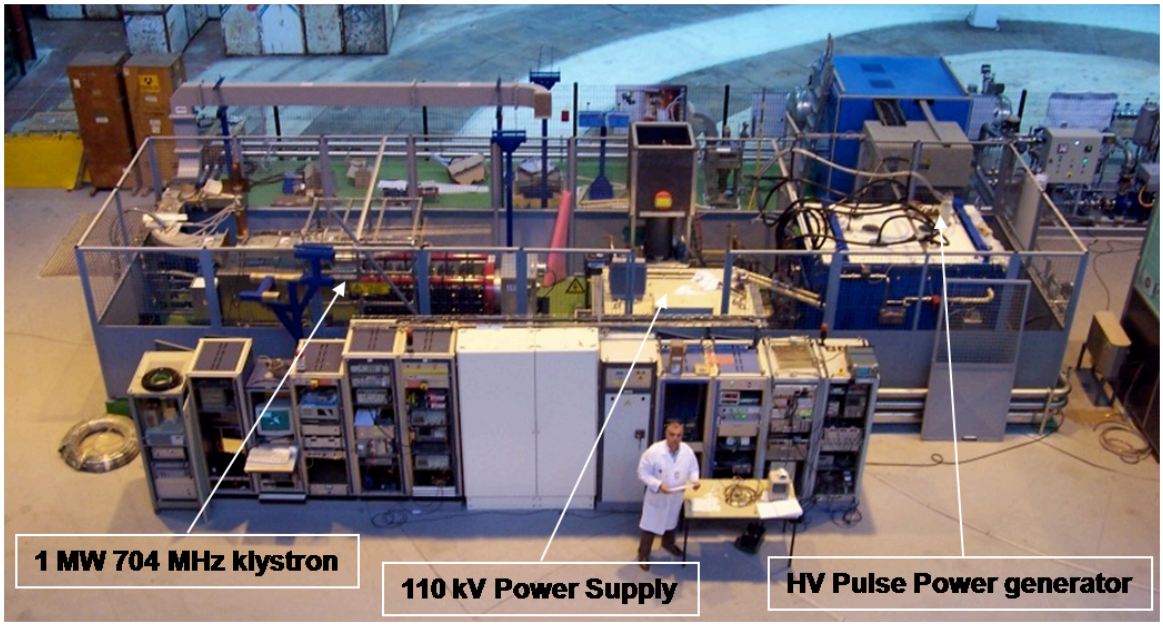

Figure 2.20: The 704 MHz high power RF test area

The klystron output is connected to a circulator and a 20 m long WR1150 rectangular waveguide line extending to the Cryholab. In March 2009 the 110 kV power supply was damaged after a series of breakdowns. The design of the transformer was modified to reduce the voltage between the primary and secondary windings. The transformer had to be rebuilt, and the repaired and upgraded power supply was only available in December 2009.

2.8.2. RF Pulse generation and control

One of the main goals of the experimental program is to demonstrate the Lorentz force detuning compensation of the beta 0.5 cavity for Eacc in the 10 to 12 MV/m range. Since the cavity is not loaded with beam, a flat top signal has to be generated to simulate the beam pulse. An RF power pulse of the shape shown on figure 2.21 can be used. If P is the forward power needed to generate the nominal accelerating field Eacc in the steady state, a pre-pulse 4P in power and $\tau \ln 2$ in length can be used to bring the cavity field to the same value. In the top part of figure 2.21 are also represented the resulting field achieved in the cavity if driven with a 2 ms rectangular pulse of amplitude P (Eacc in the steady state) and 4P (2xEacc in the steady state).

This pulse manipulation is made at a low level. The pulse is amplified to provide the drive signal to the klystron. An analog amplitude control loop ensures the stability of the klystron output power. Due to the klystron characteristics, the fast variation of the drive pulse to produce this 4P to P step in forward power generates a phase shift at the klystron output.

An analog phase control feed forward has been developed around an RF phase comparator chip commercially available to compensate for this fast phase shift. The residual phase shift during power switching is reduced to a few degrees. The advantage of having a phase

compensated forward signal on the cavity is that one can measure directly the cavity voltage phase variations on the cavity pickup output signal.

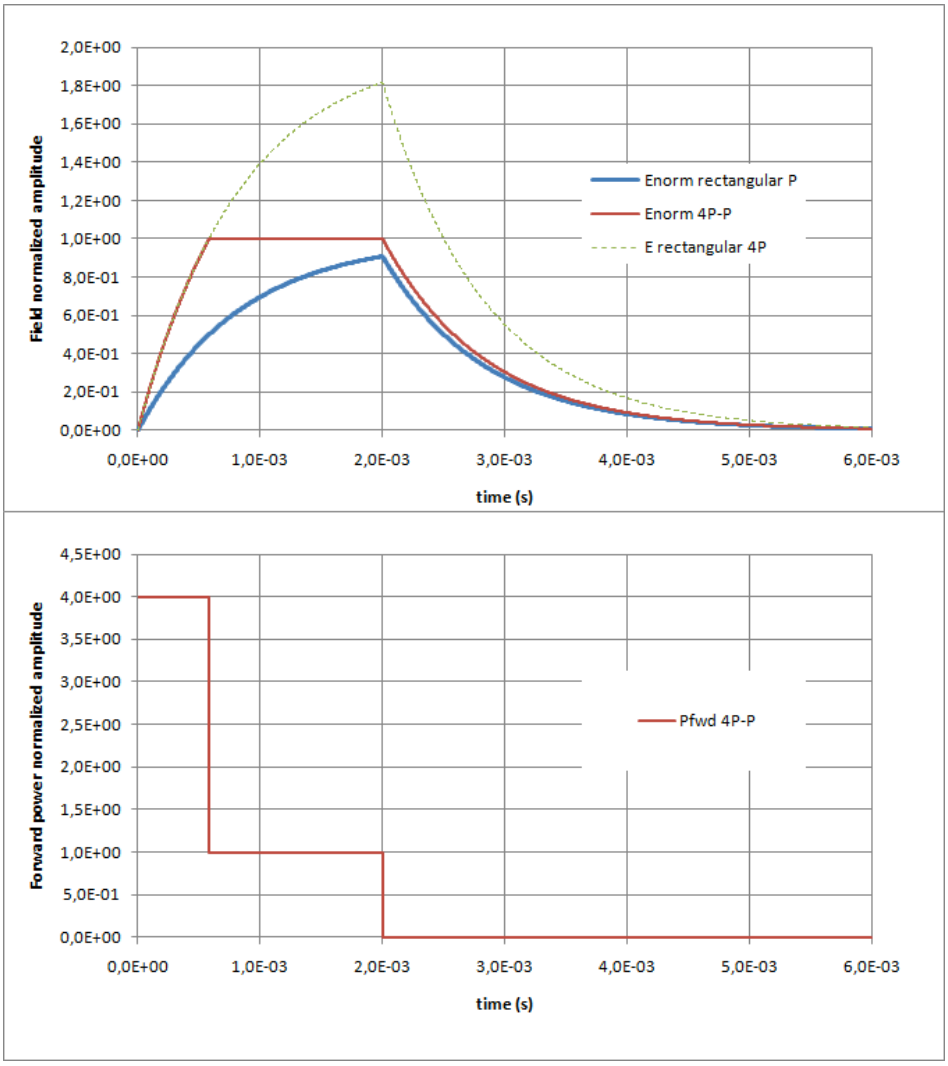

Figure 2.21: Time variation of the field in the cavity for three different forward pulses in the 5-cell cavity not experiencing LFD (top). Time variation of the forward power in the 4P-P mode used to generate the flat top (bottom).

2.8.3. Power coupler performance

The power coupler has been conditioned in travelling wave mode on the test bench beforehand [2.9]. Processing in standing wave mode has been only partially done due to the breakdown of the HVPS in 2009. The processing on the cavity in the superconducting state has first been done in 2009 with a spare HVPS, at a reduced duty cycle, but with full peak power.

3.8.3.1. Low duty cycle processing

Most of the conditioning was first done with the cavity tuned at 702.660 MHz (“zero” position of the tuning system) while the RF source was operating at 703 MHz. The initial power ramping was done with very short pulses (50 μs, 5 Hz), then widening the pulse from 100 μs

to 1 ms. It was also decided to limit the forward power to 500 kW which is enough to carry out all the experiments on the cavity at maximum accelerating gradient even using the 4P-P scheme. The same conditioning was repeated with the cavity tuned to 703 MHz, but with less than 90 kW to avoid cavity quenches.

The next step was to use the 4P-P scheme with the cavity tuner at 703 MHz at 1.8 K, to be able to lengthen the RF pulses from 1 ms to 2 ms. This was done to enable the first LFD measurements on the cavity at a 5 Hz repetition rate, so the 4P pre-pulse was set to a peak power of 84 kW, 20 kW for the flat top. This was increased up to 164-41 kW pulses to achieve the maximum field in the cavity.

2.8.3.2 High duty cycle performance

The upgraded 110 kV 2.4 A HVPS was installed at the end of 2009. The conditioning with 2 ms, 50 Hz pulses was done with the detuned cavity, in order to reach the maximum power handling capability of the coupler and study the efficiency of the He cooling circuit. Cold He gas is drawn from the Cryholab phase separator in which the operating pressure is between 1140 and 1180 mbar. It is fed to the coupler He inlet at the cavity side through simple tubing on which the temperature is monitored. Three spiral channels run in parallel in the double wall of the outer conductor from this common inlet to a common outlet, also located in the cryostat insulation vacuum. The warmed up gas is then fed to an external heater connected to the general He gas return of the facility, a few mbars above atmospheric pressure. A controlled valve and a flow-meter are located downstream the heater and allow to get a constant gas flow.

The coupler was operated at 1 MW forward power at 50 Hz 2 ms for 7 hours in a row with stable cryogenic conditions with a He gas flow of 0.6 m^3/h (measured at atmospheric pressure and room temperature). In this case the cavity was detuned in order to prevent the cavity from quenching: the quench field would be reached in only 220 μs if the cavity had been on tune.

Preliminary measurements of the He cooling efficiency have been carried out.

Conduction losses (RF off): after leaving the coupler without He counter-flow, switching on the He coupler cooling reduces the cryogenic losses at 1.8 K. A calibrated adjustable heater is used to compensate for this gain and keep the He pressure constant. Once the thermal steady state is reached, the power dissipated in the heater then corresponds directly to the reduction in cryogenic losses brought by the cooling circuit. With a flow of 0.6 m^3/h it removes 16.8 W from the conduction losses of the power coupler on the 1.8 K circuit.

RF losses at 10% RF duty cycle: The same heater compensation method is used to estimate the losses caused by RF dissipation only, at a constant cooling flow of 0.6m^3/h. The switching of the RF from 1 MW peak to 0 is compensated by a heater power of 12.3 W. This is consistent with a second measurement done by switching the RF from 500 kW peak power to 0, compensated by a heater power of 6.3 W. The antenna is water cooled, and the maximum water temperature increase observed between the inlet and outlet is 3.5 degrees. power level. This includes the air side of the coupler antenna, and is given for a water flow of 1.5 l/min. The corresponding dissipated power is 367 W. This small temperature increase implies that, at first order, the radiation losses from the antenna are independent of the RF.

Since the resonant frequency of the cavity and the RF source differ by 340 kHz during this measurement, the standing wave pattern in the power coupler is shifted by λ/4 with respect to the nominal case where the cavity is on tune. The window position with respect to the antenna tip has been defined in order to get a minimum electric field in the ceramic having in mind this nominal case (fig. 2.22, top). In the experimental conditions we are discussing

here, the ceramic disk is at the maximum electric field location. More important is that the maximum magnetic field is located near the RF gasket between the cavity and the coupler, which is also a possible driver for higher losses, or less efficiently cooled power dissipation (fig. 2.22, bottom).

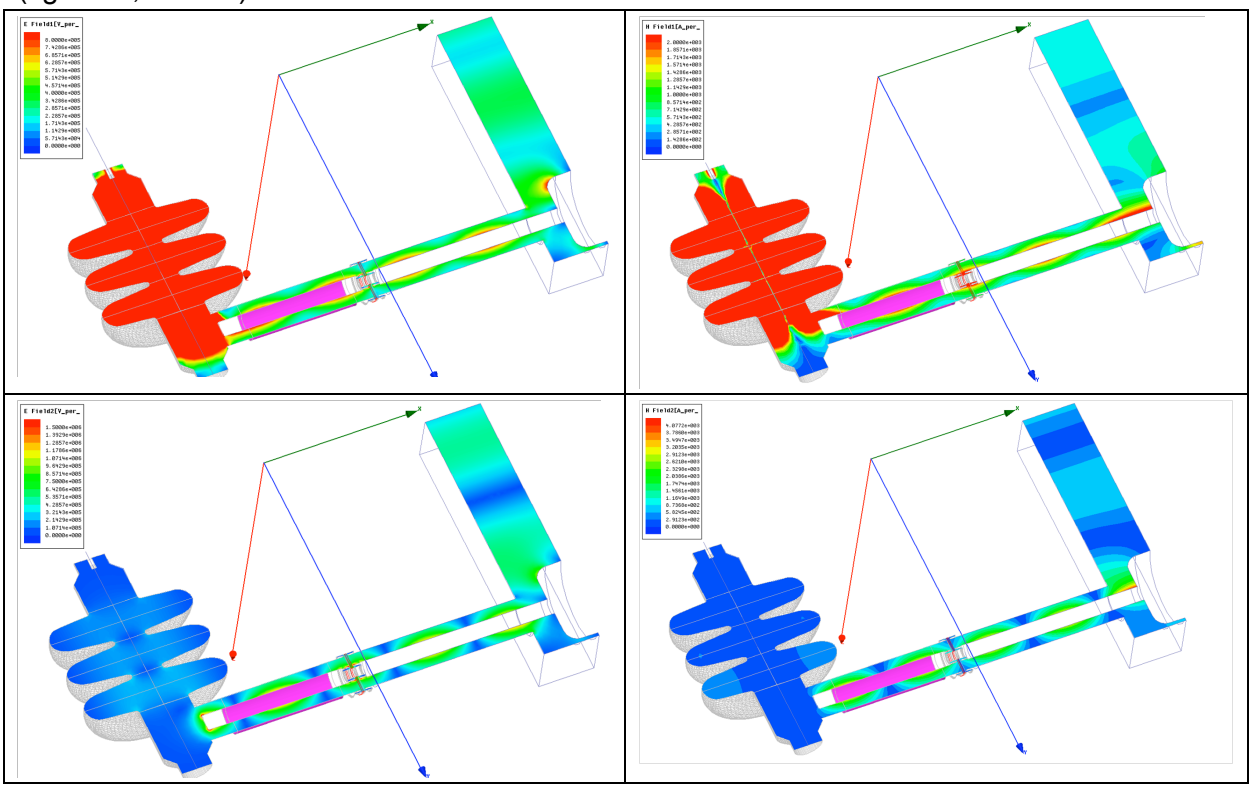

Figure 2.22: Electric (left column) and magnetic field (right column) standing wave pattern simulated with HFSS. The top line represents the tuned cavity case, the color scale has been chosen to emphasize the fields in the power coupler. The bottom line represents the case where the cavity is far from resonance and corresponds to the actual experimental conditions discussed here.

More measurements are necessary to understand if modifying the field pattern is changing the situation. This requires going very close to the cavity resonance to scan a sufficiently large range of the field maxima in the coupler. Running this measurement using rectangular pulses with a constant peak power of 50 kW would prevent the cavity from quenching. However, the average forward power being reduced by a factor of 20 down to 5 kW, the resultant RF dissipation would experience too large a reduction to be measured with a sufficient accuracy in Cryholab. An alternative way is to use an IOT in CW mode to keep the average forward RF power around 50 kW. We are in the process of commissioning an 80 kW IOT in the coming months to perform this measurement.

Air-side arcing events

While operating above 800 kW, an attempt to cool the air side of the ceramic by blowing nitrogen instead of air into it, lead to strong arcing activity in the RF window area and to a lesser extent in the coaxial guide between the window and the doorknob. The photomultiplier on the vacuum side was triggered by those arcs, so the window was protected from

destruction thanks to the fast response time of the electronics. No pressure rise in the coupler vacuum was linked to those events. The arcing phenomenon disappeared immediately when the nitrogen flow was interrupted. Visual inspection revealed copper was sputtered onto the ceramic, near the inner choke region. After warming up of the cryostat the ceramic was cleaned in-situ applying locally low concentration nitric acid taking care not to contaminate the region near the braze joint. The nitric acid concentration was defined beforehand on ceramic samples smeared with copper. The operation could not remove all copper residues. However, the window could be operated normally afterwards. It should be noted that the full day test at 1 MW full duty cycle was carried out after this incident.

2.8.4. Cavity behavior in pulsed mode

The last preparation of the cavity has been efficient since the field emission that was observed in the previous tests disappeared in the final configuration. This means the field emitters have been removed from the surface and the final assembly with the FPC was done without contaminating the cavity.

The maximum Eacc of 18.5 MV/m has been obtained when the RF is pulsed at 5 Hz, with 500 μs long pulses. For longer, 2 ms pulses, the cavity quenches at 16.6 MV/m, which is comparable to the maximum gradient of 16 MV/m obtained in CW mode during the low power tests.

3.8.4.1 Lorentz detuning

The interesting parameters for the operation are the amplitude and phase stability of the cavity voltage during the beam pulse (“flat top”). The pulse duration of 2 ms is of the same order of magnitude as the mechanical mode periods we expect to be detuning the cavity, observed on the piezo voltage-to-detuning transfer function. A single RF pulse cannot bring the mechanical system into its steady state, even less if the mechanical modes have a high quality factor. The repetition of the RF pulses at the frequency f_{rep} will generate a different cavity behavior if the mechanical modes have not fully decayed between two RF pulses. For instance, a typical mode resonating at 200 Hz with a quality factor of 100 has a decay time of 160 ms. It will not decay between two successive pulses at f_{rep} = 50 Hz separated by only 18 ms, so we expect the detuning effect of successive pulses to interfere with each other. In the most common case where the mode frequency is not a multiple of f_{rep} , a constructive interference will not occur, eventually leading to a steady state, only perturbed by microphonics.

In order to carry out measurements, the phase and amplitude of the forward, reflected and cavity pickup signals are recorded by the LLRF crate designed and built at CERN [2.10]. The following measurement at f_{rep} = 50 Hz with increasing values of the gradient in the cavity shows the amplitude and phase variation of the cavity voltage from the start of the pulse to the cavity field decay. The static tuning can be adjusted using the motor of the tuning system or by applying a DC voltage to the piezo the latter was used here. For this data set, the cavity was tuned at 703 MHz for the lowest gradients (fig. 2.23). The accelerating field measured at the end of the filling time ranges from 9.8 to 14.3 MV/m in this example.

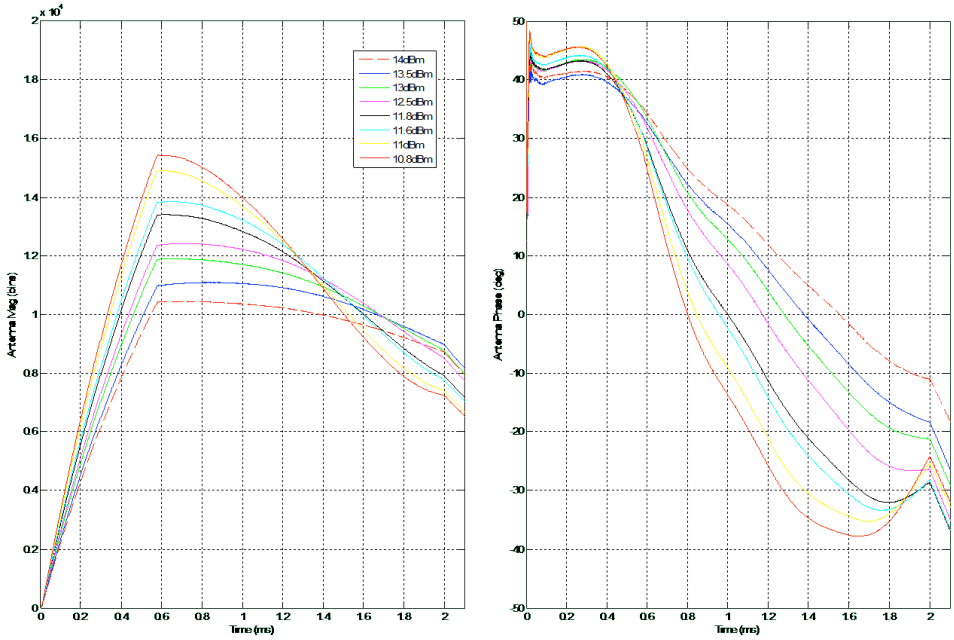

Figure 2.23: Cavity voltage amplitude and phase during the RF pulse for different forward power levels. Piezo compensation is off.

The peak-to-peak phase variation during the flat top from this data is shown on figure 2.24 as a function of the square of the accelerating field at the end of the filling time.

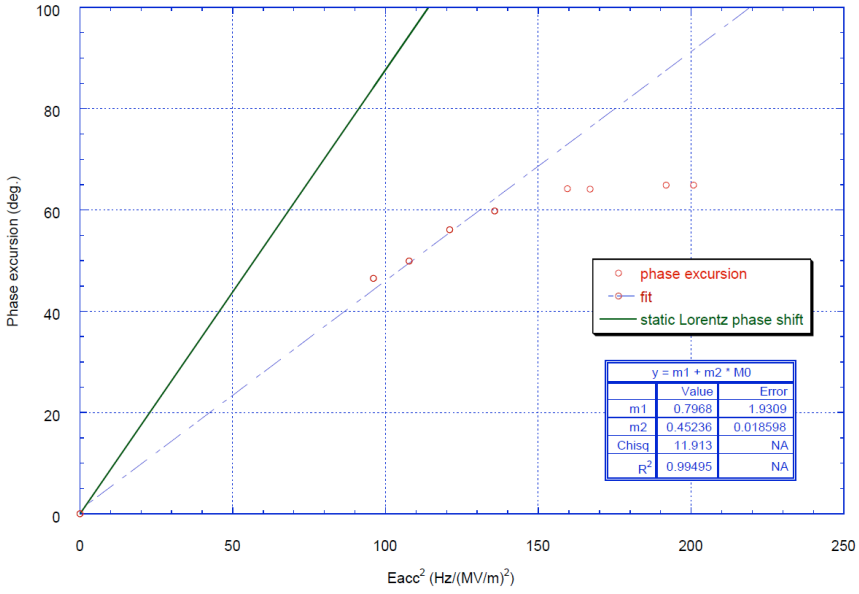

Figure 2.24: Peak-to-peak phase modulation during the pulse

The equivalent phase shift corresponding to the static detuning is reported for comparison only: KL= -3.8 Hz/(MV/m)^2. The dotted line is a fit to the first 4 data points, and gives an upper boundary for the phase excursion in all cases. The comparison of the two lines simply means that if an estimation of the phase shift was done using the static KL, it would

overestimate the measured data by a factor of 2 approximately. For the highest Eacc value in the data, the detuning is so strong that the field is heavily reduced during the pulse. This in turn reduces drastically the radiation pressure and the cavity starts to spring back even before the end of the pulse, which can be clearly observed on the cavity phase signal (fig. 2.23, plain red curve, for instance).

The field at the end of the filling time is only weakly affected by the Lorentz detuning. This can be seen by comparing E^2_{acc} at the end of the filling time against the peak forward power during the pre-pulse (fig. 2.25). This is mostly due to the slow mechanical time response of the cavity which is of the order of 1 ms.

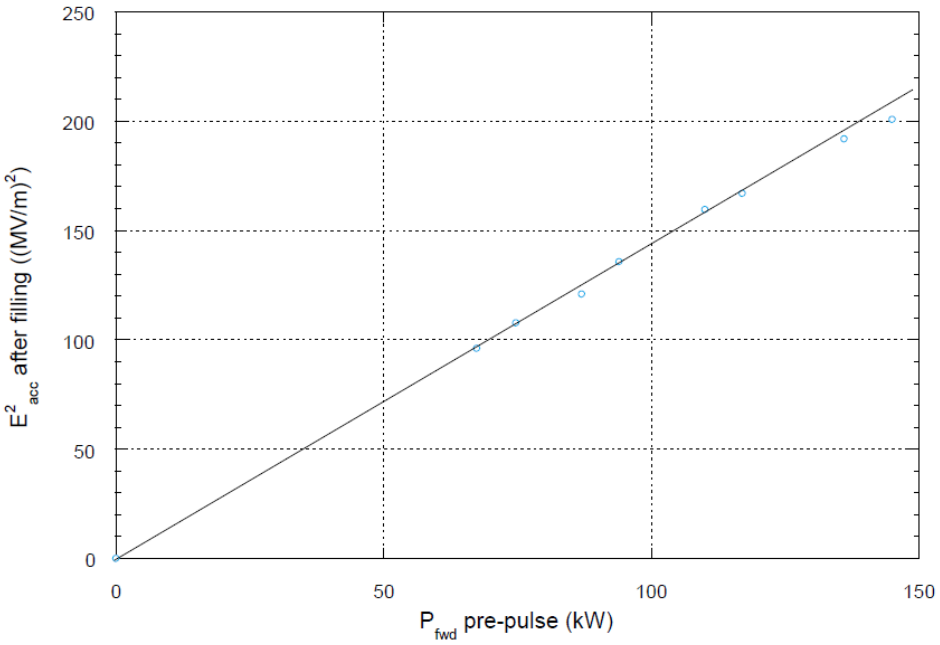

Figure 2.25: Measurements of the E^2acc at the end of the filling time with respect to the pre-pulse forward power in the 4P-P scheme

2.9. LORENTZ FORCE DETUNING COMPENSATION

The compensation of Lorentz forces is done by driving the piezo actuator, mainly finding the correct combination of pulse amplitude, length, and trigger position. This was done manually, by observing the phase and amplitude of the cavity pick-up signal on a real-time spectrum analyser, which performs I/Q demodulation of the signal. An optimization was done by changing the piezo drive pulse parameters to minimize the modulation of phase and amplitude during the flat top. The compensation has been achieved for different combinations of accelerating gradients and repetition rates. The forward, reflected and cavity pickup signals are recorded by the LLRF crate. The example below is for E_{acc}=13 MV/m and a Frep=50 Hz, the RF pulses are 2 ms long.

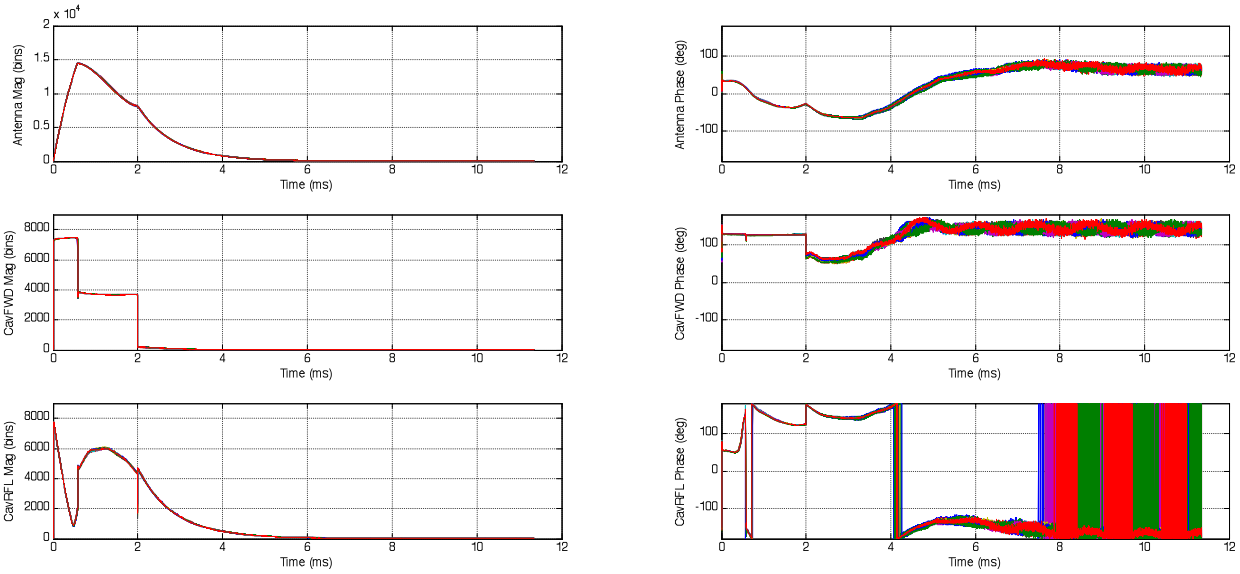

Figure 2.26: Amplitude (right) and phase (left) of the cavity pick-up antenna (top), cavity forward (center) and cavity reflected signals, without compensation.

The recorded signals on the CERN crate are shown first without piezo compensation (fig. 26 and fig. 2.27). A zoom on the cavity pick-up signal shows the effects of the detuning on the amplitude which drops by 45% and the phase which is modulated within +/- 25 degrees during the 1.4 ms flat top.

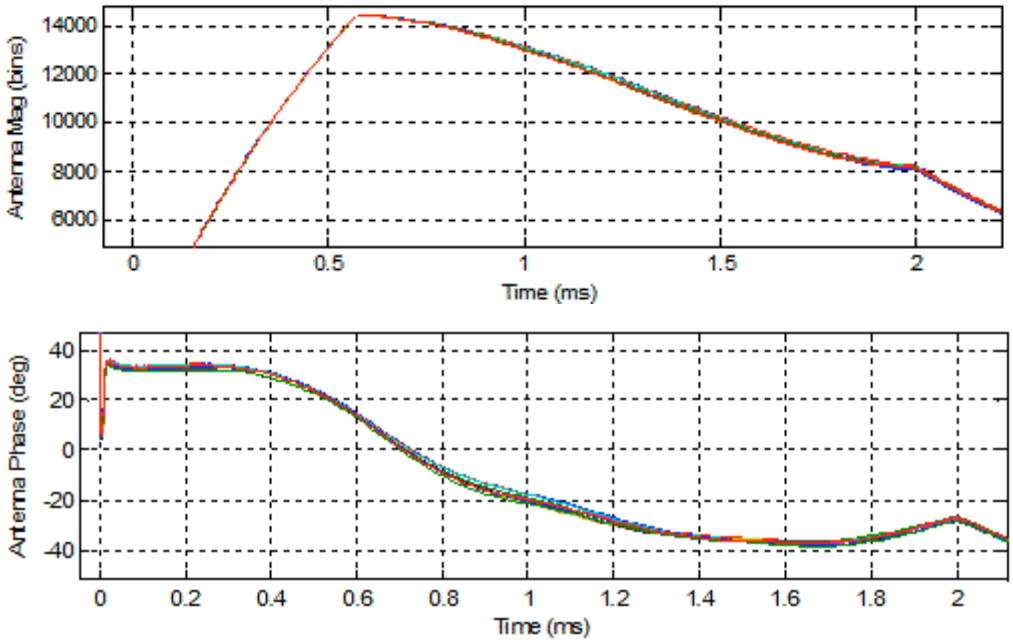

Figure 2.27: zoom on cavity pick-up amplitude and phase signal, piezo is off.

An example of the piezo drive signal for compensation is shown on figure 2.28: it starts 940 μs ahead of the RF pulse.

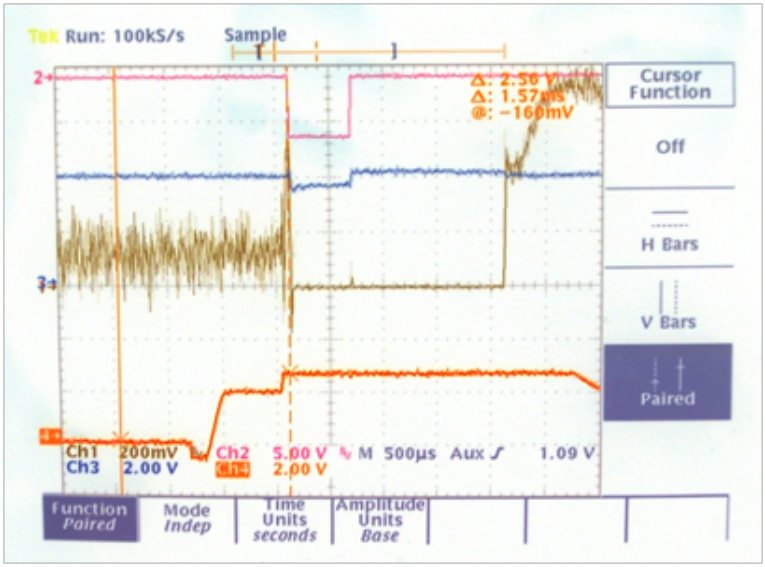

Figure 2.28: Piezo drive signal (orange at the bottom) scaled by a factor 100 (1V corresponds to 100V on the piezo). The RF pulse starts at the vertical dotted line

The result on the cavity voltage is a reduction of the amplitude variation to only 1.4% and the phase variations are within +/- 8 degrees during the flat top. The reproducibility of the signal is good, 8 pulses are superimposed in figure 2.29.

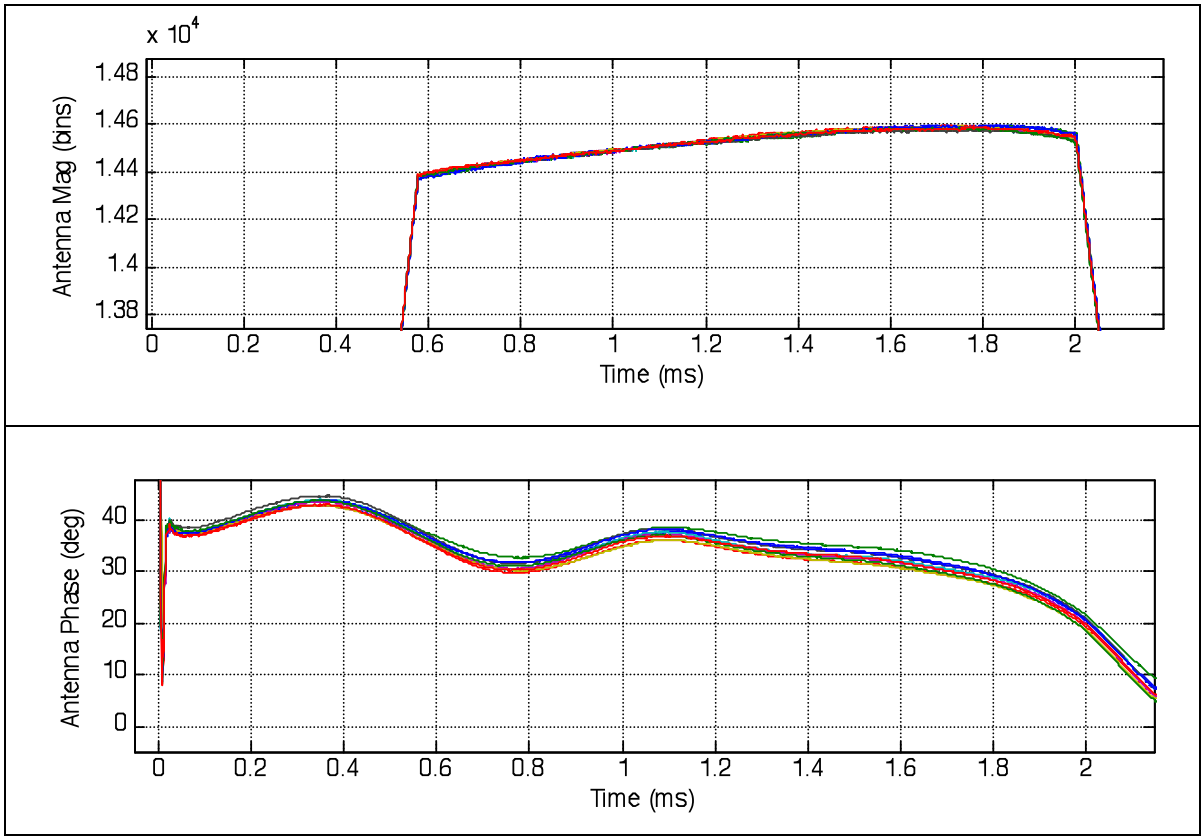

Figure 2.29 : zoom on the cavity pick-up amplitude and phase, with piezo compensation of LFD at f_{rep} = 50 Hz

The previous example corresponds to the highest accelerating field (13 MV/m) that we have attempted to compensate for the LFD. We have applied Fourier analysis on the measured cavity signals, with and without compensation respectively. But the fact that the cavity phase can only be measured for several ms before being dominated by noise during the cavity field decay limits the frequency resolution that can be achieved, typically 200 Hz. A continuous RF signal feeding the cavity is needed to cope with this. A much better measurement will be possible after the IOT connection to the Cryholab experiment.

2.10. PIEZO SIGNAL ANALYSIS

An alternative way to observe cavity mechanical excitation is to measure the piezo signal. Measurements of the piezo voltage have been carried out with a computer equipped with a data acquisition board with a sampling rate of 10 kHz.

2.10.1. Time Domain signals

Figure 2.30 shows the piezo voltage when the cavity is driven at 12 MV/m with 2 ms pulses repeated at 4.17 Hz. No attempt to compensate for the LFD is made here. The 240 ms pulse spacing allows for mechanical mode decay.

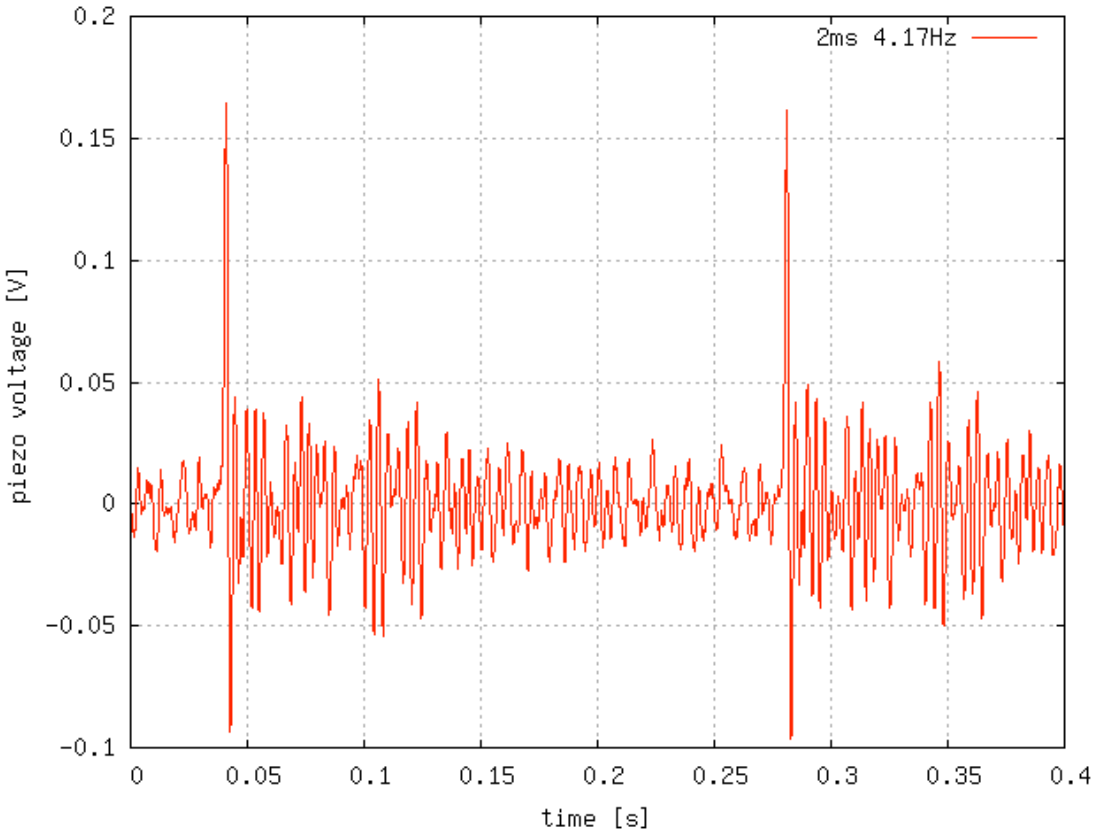

Figure 2.30: Piezo excitation due to Lorentz forces on the cavity at 12 MV/m, 2 ms rectangular RF pulses, 4.17 Hz repetition rate.

When increasing the repetition rate to 50 Hz with no other change in the setup, several mechanical modes have no time to decay between RF pulses (fig. 2.31) and the cavity experiences forced mechanical oscillation at all times. However, the effect of successive pulses does not build up in a constructive way. The peak to peak excursion of the piezo voltage is the same as for the 4.17 Hz repetition rate, and the mechanical oscillation is very stable.

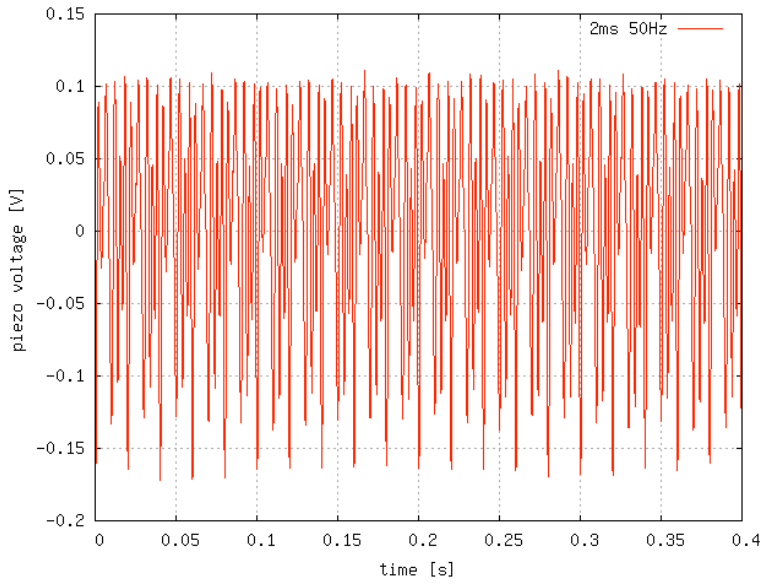

Figure 2.31: Piezo excitation due to Lorentz forces on the cavity at 12 MV/m, 2 ms rectangular RF pulses, 50 Hz repetition rate.

This type of measurements were repeated for every available pulse spacing of our timing system, namely 600, 480, 240, 120, 60, 40, and 20 ms, and we never observed any instability build-up on the piezo signal. This observation does not exclude the possibility that for specific values of the pulse spacing, or more generally RF pulse spectrum, a mechanical instability could grow.

2.10.2. Spectral analysis

The microphonics result from the mechanical excitation of the cavity by its environment. The observation of the piezo signal can reveal part of the cavity mechanical excitation, but differ from a proper microphonics RF measurement. However such a measurement is necessary to separate the contribution of environment and Lorentz detuning in any spectrum shown later. The spectrum of the piezo signal when RF is off is shown in figure 2.32. The data correspond to a 1 minute recording. The harmonics of the mains at 100 and 150 Hz dominate the spectrum. More interesting is the presence in fig. 2.32 of the low frequency signals at 44 Hz and 75 Hz which could not be observed on the piezo drive-to-detuning transfer function. These could be either a mechanical mode of the mechanical system not associated to any detuning of the cavity, or environmental noise (pumps, cryogenics).

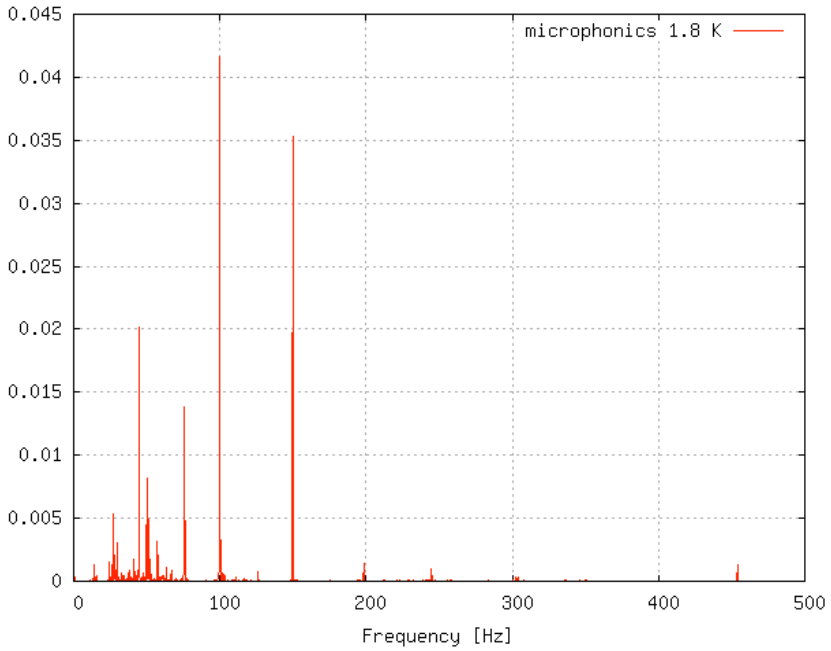

Figure 2.32: Power spectrum of the piezo signal measurement at 1.8 K, RF is off

The power spectrum of the piezo signal generated by a single 2 ms rectangular RF forward pulse is shown in figure 2.33. The main contribution comes from the mode at 125 Hz. This mode was observed in the piezo voltage-to-detuning transfer function, but was not identified as a major contribution to the cavity detuning (fig. 2.19) in contrast to the modes between 200 and 300 Hz.

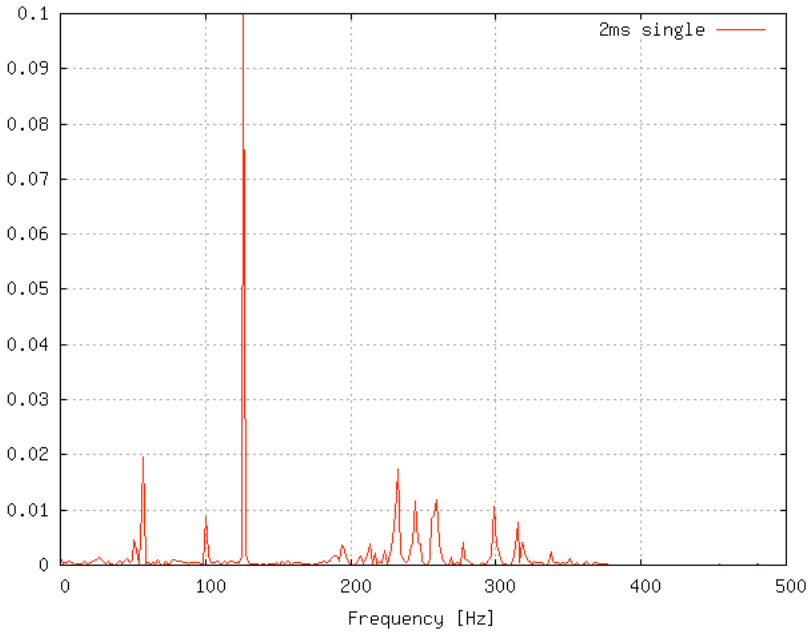

Figure 2.33: Power spectrum of the piezo signal for a single 2 ms rectangular pulse

The 100 Hz line observed in the microphonics spectrum is also present in figure 2.33, but only represents a small fraction of the frequency content of the measurement

The cavity was also driven with a 4P-P 2 ms pulse at 50 Hz with a maximum accelerating field of 14.5 MV/m and the results are somewhat different. Figure 2.34 shows the piezo response to this specific excitation. The first 0.55 s on the plot correspond to forced oscillations due to the Lorentz force. The RF is then switched off and the system is oscillating freely. The excited mechanical modes decay for about 2 seconds, then the remaining oscillations corresponds to the microphonics.

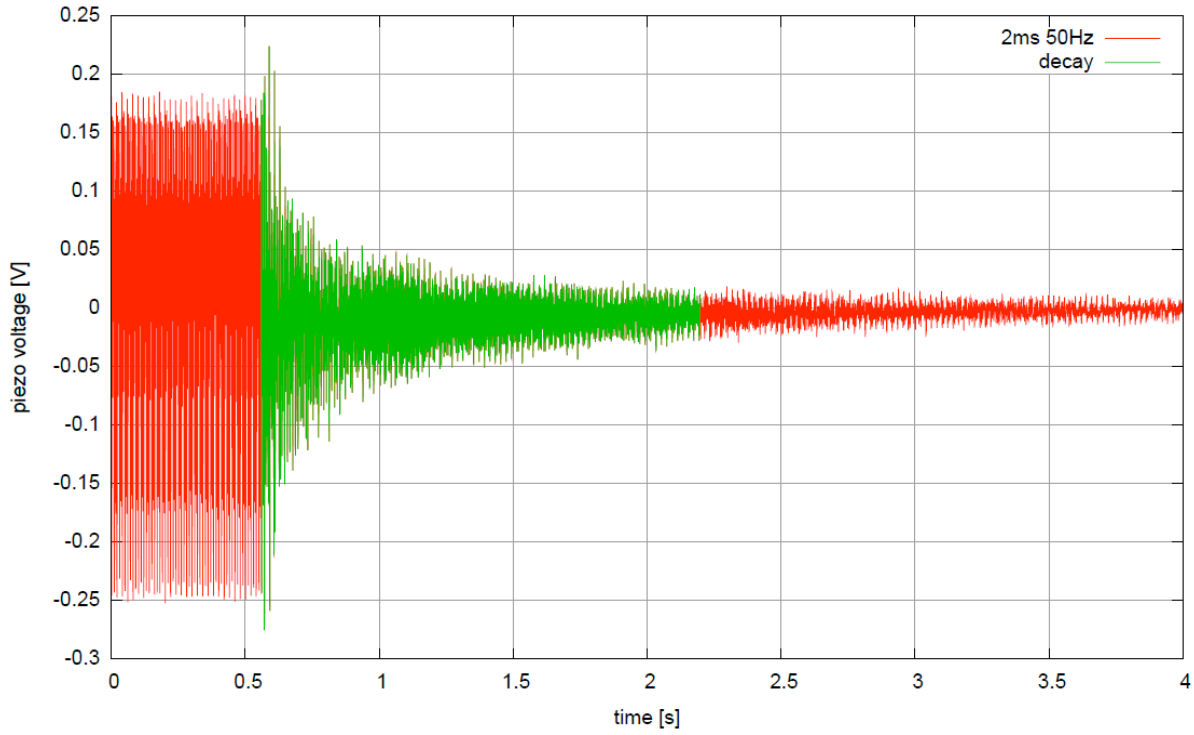

Figure 2.34: Piezo signal due to 50Hz excitation for the Lorentz force followed by free oscillation of the mechanical system

The power spectrum of the decaying part of the data marked in green in figure 2.34 is shown in figure 2.35. In this RF pulse configuration, not only the LFD is very strong, but the repetition rate of 50 Hz has excited the cavity modes lying close to its harmonics, at 198 and 301 Hz, while the 125 Hz mode, still present in the spectrum has only a small contribution.

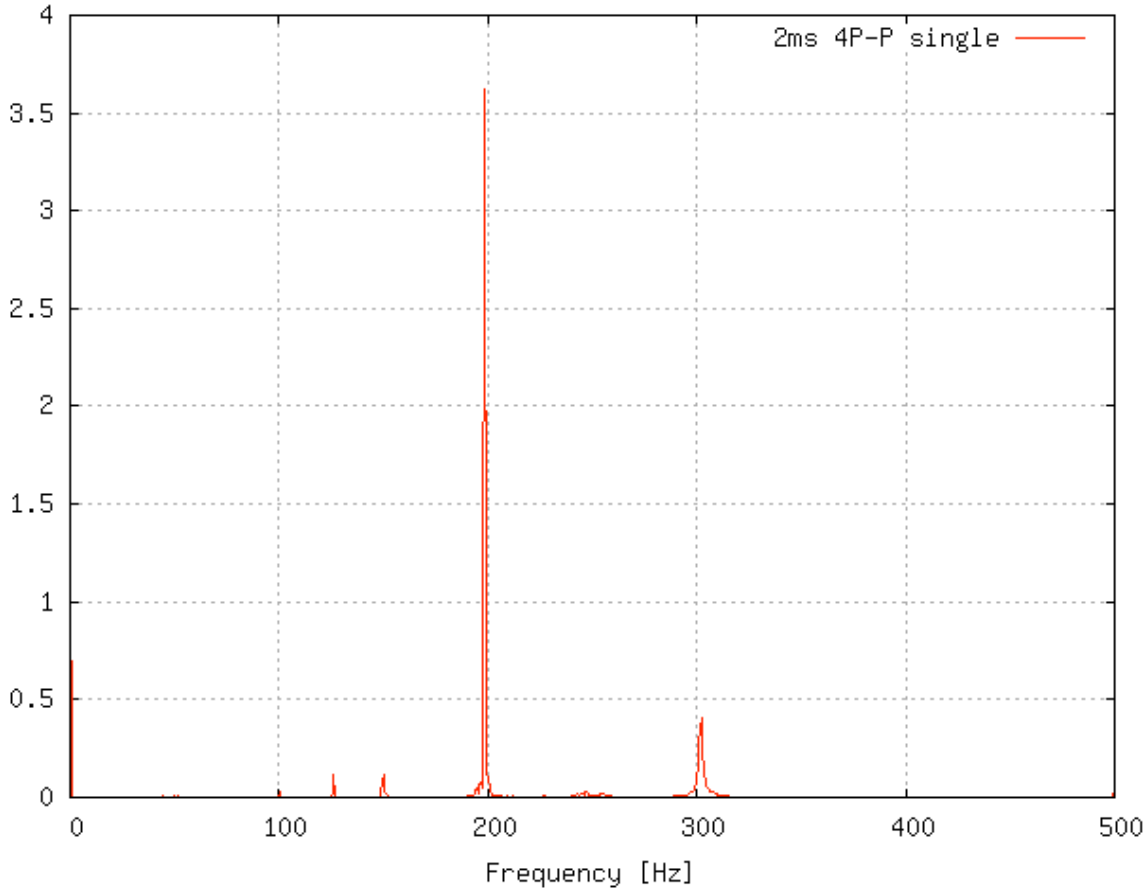

Figure 2.35: Piezo signal power spectrum using a 4P-P pulse, from the decay signal of fig. 2.34

Using the same decay signal extending now for 3.2 s a higher spectral resolution can be achieved. First estimates on the mechanical quality factors can be extracted from the half width of the main peaks: the Q factor of the 198 Hz and 301 Hz modes are of the order of 400 and 300 respectively.

2.11. CONCLUSION

The main parameters concerning the operation of the Saclay beta 0.5 704 MHz cavity have been measured experimentally, in the foreseen operating conditions, including the high duty cycle required for a high intensity proton injector. The medium beta cavities are sensitive to Lorentz force detuning, and pulsed operation does excite mechanical modes which have no time to decay at a repetition rate of 50 Hz. Still, this fact did not prevent the fast tuner from obtaining a sufficient LDF compensation, meaning the residual phase and amplitude are within the capabilities of a typical LLRF system to deal with.

A better understanding of the excitation of mechanical modes by the Lorentz force requires additional measurements in CW mode with a higher power than was is available at the test area. An 80 kW 704 MHz IOT is being installed next to the Cryholab facility in order to carry out these measurements. The possibility to excite the main mechanical modes into steady

state by modulating the RF source, and observe their individual decay thanks to the CW regime can bring experimental evidence of repetition rates that should be avoided for instance.

2.12. REFERENCES

[2.1] O. Napoly et al., "The CARE accelerator R&D programme in Europe", Proc. of PAC05, Knoxville (2005)
[2.2] H. Safa, "Superconducting proton linac for waste transmutation", Proc of 9th SRF workshop, Santa Fe (1999)
[2.3] D. Barni et al., "Status of the high current proton accelerator for the TRASCO program", Proc. of EAPC02, Paris (2002).
[2.4] G. Devanz et al., "Stiffened medium beta 704 MHz elliptical cavity for a pulsed proton linac", Proc. of SRF07, Beijing (2007).
[2.5] G. Devanz et al. "Experimental characterization of a 700 MHz β=0.47 5-cell superconducting cavity prototype for pulsed proton linac", Proc. of EPAC08, Genoa (2008).
[2.6] H. Saugnac et al., "Cryogenic installation status of the CRYHOLAB test facility", Proc. of the 10th SRF workshop, Tsukuba (2001).
[2.7] J. Plouin,"Magnetic shield for the 5-cell HIPPI superconducting cavity", internal report (2010).
[2.8] S. Chel et al. "New 1 MW 704 MHz test stand at CEA-Saclay", Proc. of EPAC08, Genoa (2008).
[2.9] G. Devanz et al., "Conditioning of the 1 MW 704 MHz Coaxial Power Coupler", proc. of SRF09, Berlin (2009).
[2.10] D. Valuch et. al, report on CERN LLRF crate : https://edms.cern.ch/file/994198/1/MeasurementSetupForCavityDetuning-Valuch-2009-02-01.pdf